ACTA IMEKO
ISSN: 2221-870X
September 2025, Volume 14, Number 3, 1 - 17

A model for the population dynamics of plants under extensive livestock grazing

Octavio Augusto Bruzzone[1], Luca Rossini[2], Daiana Vanessa Perri[1], Marcos Horacio Easdale[1]

[1] *CCT Patagonia Norte, CONICET, San Carlos de Bariloche, Rio Negro, Argentina*
[2] *Service d'Automatique et d'Analyse des Systèmes, Université Libre de Bruxelles, Av. FD Roosevelt 50, CP 165/55, 1050 Brussels, Belgium*

ABSTRACT
Extensive livestock production on rangelands involves continuous biomass extraction, as various plant species serve as food for different animal populations. Unlike agricultural systems, rangeland biomass extraction reduces plant size without their complete removal, leading to more complicated management strategies. Mathematical models could predict where plant biomass is available, to relocate animals accordingly, but the current state of the art offers plant population models with a single variable, confusing growth rate, fitness, and carrying capacity. This study addresses this limitation through a model that divides plant populations into two state variables: i) total biomass (B) and ii) the number of individuals/vegetation cover (N). Biomass follows a standard logistic population dynamic constrained by the carrying capacity of the ecosystem, while N represents population spread and resource acquisition. The model integrates Schaeffer and Noy-Meir logistic population models with biomass extraction and includes a seeding term (S) to account for human interventions. Results showed that system stability and equilibrium depend on the efficiency parameter (N_h), which links B and N. Higher N values reduced the system's maximum yield under biomass extraction, highlighting the trade-off between vegetation cover and biomass productivity. This model provides a promising alternative for describing rangeland dynamics under extensive livestock production.

Section: RESEARCH PAPER

Keywords: grazing; biomass; resource capture efficiency; herbivory; cattle; pastoralism; semi-arid environments

Citation: O. A. Bruzzone, L. Rossini, D. V. Perri, M. H. Easdale, A model for the population dynamics of plants under of extensive livestock grazing, Acta IMEKO, vol. 14 (2025) no. 3, pp. 1-17. DOI: 10.21014/actaimeko.v14i3.2039

Section Editor: Elisabeth Costa Monteiro, Pontifical Catholic University of Rio de Janeiro, Brazil

Received December 19, 2024; **In final form** July 30, 2025; **Published** September 2025

Corresponding author: Octavio A. Bruzzone, e-mail: bruzzone.octavio@inta.gob.ar

ABBREVIATIONS

B - Total biomass
N - Total number of plant individuals/vegetation cover
S - Seeding
r - Growth rate
r_b - Biomass growth rate
r_n - Individuals' growth rate
K - Carrying capacity
K_B - Biomass carrying capacity
Z - Average size of individuals
Z_0 - Average size of individuals to achieve net population growth
Z_min - Minimum size of individuals
t - Time
C - Total extraction rate of biomass
L - Extraction rate by livestock
H - Extraction rate by wild herbivores
a - Herbivores efficiency
h - Herbivores handling time
db_max - Maximum derivative of the biomass function
B_x - Value of B at which db_max occurs
db_min - Minimum sustainable derivative of the biomass function
B_min - Value of B at which db_min occurs
B_st - Value of B where the system is in a stable equilibrium.

1. INTRODUCTION

Mathematical models are powerful tools for understanding the processes of growth, decline, colonisation, and extinction in biological populations [1], [2], as well as for describing species interactions such as predator–prey dynamics and competition [3].

Over the years, these models have been adapted to agricultural and farming systems to describe the continuous extraction of resources. Such models, commonly called "bioeconomic models", have been widely applied to rangeland ecosystems worldwide. Notable examples include the works of Petit [3], Zhang & Smith [4], Ritten et al. [5], and Hanson & Ryan [6].

Extensive livestock production, which relies on arid and semi-arid rangelands, presents unique modelling challenges. Unlike intensive agricultural systems, where human actions drive vegetation and animal dynamics [7], extensive systems are characterised by minimal human intervention and indirect removal of biomass by different pools of organisms [8]. Natural resources, such as grasses and shrubs, are seldom replaced, and the system is maintained with extremely low external inputs of energy and nutrients. Reynolds et al. [8] have described two key features of these systems: *i)* plant populations are subject to minimal management, and *ii)* animal populations are affected by human actions. These single-stock models typically describe plants through a single variable, such as green biomass or aboveground net primary production [9], [10], and often neglect interactions with the surrounding environment, such as soil nutrient availability.

The mathematical representation of extensive livestock systems is often based on simple bioeconomic models, such as single-stock logistic growth or Volterra-Lotka-like predator–prey models [11]. Biomass extraction within these models is commonly described in two ways. Schaeffer proposed to modify the logistic growth equation by including a constant extraction term, either as a fixed amount or as a fixed proportion of the standing biomass, as in Holling's type-I functional response. Noy-Meir, instead, proposed nonlinear functional responses that explicitly link extraction rates to resource availability. In this work, we refer to these modelling practices as the Schaeffer-type and Noy-Meir-type families, respectively. The most influential contributions on this topic were given by Noy-Meir [10]–[14] and, more recently, by Fort et al. [15] and Dieguez Cameroni & Fort [16].

While single-variable models are analytically simple and useful for theoretical studies, they have significant limitations. For instance, they fail to account for population components such as age and size structure, phenological status, and spatial distribution, and they also assume homogeneity among individuals, oversimplifying the system. As a result, single-variable models reduce the complexity of the problem but lack the precision required by practical applications. Increasing the number of variables (e.g., by incorporating plant–nutrient interactions) could improve accuracy, but it also dramatically increases the dimensionality of the system. An additional challenge is the uneven distribution of plant biomass and resources (e.g., nutrients, water) within the environment [17], [18], which affects their accessibility to individuals.

Spatially explicit models based on reaction–diffusion equations [19] or individual-based matrices [20] have partially addressed this issue. These models often include the law of diminishing returns, which assumes that each individual uses only a limited portion of the available resources. This assumption reduces the dimensionality of the system without, but not the connection with, the bioecology of the problem [21]. This approach could be valuable for modelling extensive livestock systems.

Human interventions further complicate the mathematical description of extensive livestock. Common practices include seeding [22]–[24], replacing natural plant populations with more productive species [25], and fertilisation or irrigation to promote plant growth [26], [27]. Additionally, when animal populations exceed the habitat's carrying capacity, temporary artificial food supplies are often provided [28].

This study aimed to develop a model that describes plant population dynamics in a human-driven landscape, finding a good compromise between detail and complexity. Notably, the model aims to: *i)* describe plant populations in terms of biomass and the number of individuals, *ii)* account for continuous extraction, particularly grazing by livestock, and *iii)* incorporate limited human interventions such as seeding. While primarily designed for rangelands with extensive livestock grazing, the model is general enough to be applied to other production contexts and ecosystems with minimal modifications.

2. METHODS

2.1. Model development

2.1.1. Number of individuals and biomass

Let us consider logistic growth, the simpler model of population dynamics with density-dependence, mathematically described as:

$$\frac{\mathrm{d}}{\mathrm{d}t}N(t) = r\,N(t)\left(1-\frac{N(t)}{K}\right). \tag{1}$$

In equation (1), $N(t)$ is the biological abundance (e.g., the number of individuals of a given species per area, or the total biomass), r is the intrinsic growth rate, and K is the carrying capacity. According to the current literature [29], K can be defined in different ways. We hereby refer to "carrying capacity" as *the maximum plant biomass that the system can support at equilibrium without removal and using all resources available*. In line with most of the simple theoretical models of population dynamics, we do not explicitly include seasonality or time scales in this study, either. It is worth remarking, however, that this aspect does not affect the structure of the equation, as it leads to considering time-dependent parameters instead of constant ones.

Equation (1) is composed of two terms: an exponential term $r\,N(t)$ that multiplies the population at time t and the relative growth rate, and a second density-dependent term that moderates growth so that the system approaches K asymptotically. We can adapt equation (1) to model extensive plant populations by considering two separate state variables: biomass, $B(t)$, and the number of individuals, $N(t)$. The parameters related to biomass are hereafter denoted by the subindex b, while the parameters related to the number of individuals are denoted by the subindex n. Additionally, the total biomass should grow logistically at a rate r_b and up to a certain asymptotic value K_b, i.e., the carrying capacity with respect to the total biomass available in the environment.

The complexity of the system can be reduced by assuming that the number of individuals grows with the rate r_n without having an asymptotic value (K_n). Linking the state variables $N(t)$ and $B(t)$ helps prevent the number of individuals from growing exponentially without bounds. Empirical evidence shows that small individuals (i.e., those below a certain size threshold) are less likely to reproduce and have a higher mortality. Conversely, once individuals overtake the threshold, reproduction becomes viable, and the population can grow. Classical studies on plant demography in rangelands also suggest that competition effects, driven by plant density, can reduce seed production in pastures [30].

We define the ratio $Z(t) = \frac{N(t)}{B(t)}$ as the average size of individuals within the population. We further introduce a threshold parameter Z_0, representing the minimum average size of the individuals required for net population growth (i.e., for the birth rate to exceed the death rate). This threshold encapsulates both survival and reproductive viability: individuals smaller than Z_0 are assumed to be either non-reproductive or more prone to mortality. Accordingly, if $Z(t) < Z_0$, the population declines; if $Z(t) > Z_0$, the number of individuals increases. Based on these assumptions, the population model can be rewritten as:

$$\begin{aligned} \frac{\mathrm{d}}{\mathrm{d}t} B(t) &= r_\mathrm{b}\, B(t) \left(1 - \frac{B(t)}{K_\mathrm{B}}\right) \\ \frac{\mathrm{d}}{\mathrm{d}t} N(t) &= r_\mathrm{n} \left(\frac{B(t)}{N(t)} - Z_0\right) N(t), \end{aligned} \tag{2}$$

where now the average size of the plants $\frac{B}{N}$, and the population density $N(t)$ have a linear dependence. If the average size of the plants is lower than Z_0, the recruitment of individuals becomes negative. Otherwise, the recruitment is positive, and the number of individuals grows.

To describe the efficiency of the individuals in using resources (i.e., the average range over which an individual of the population can access resources), we introduce a new term into equation (2). This term refers to the increase of the biomass rate and to the number of individuals, following Mitscherlich's law of diminishing returns. In other words, the efficiency gained from increasing the number of individuals decreases with the population abundance.

Resource consumption is often modelled using Holling's Type II functional response [31], which is mathematically equivalent to the Michaelis-Menten enzyme kinetics model [32], albeit with a different parameterisation. Following the classical integration of functional responses into population dynamics models of Oaten and Murdoch [33], we adopt a saturating function to model resource capture efficiency. However, we simplify the formulation by using the Michaelis-Menten structure with a single half-saturation constant, rather than the separate "attack rate" and "handling time" parameters typical of Holling's model. This choice provides a parsimonious formulation that captures the essential saturation behaviour, while minimising the number of parameters and avoiding strong assumptions about the system's behaviour at low densities.

Accordingly, the model becomes:

$$\begin{aligned} \frac{\mathrm{d}}{\mathrm{d}t} B(t) &= r_\mathrm{b}\, B(t) \left(1 - \frac{B(t)}{K_\mathrm{b}}\right) \\ \frac{\mathrm{d}}{\mathrm{d}t} N(t) &= r_\mathrm{n} \left(\frac{B(t)}{N(t)} - Z_0\right) N(t), \end{aligned} \tag{3}$$

with $N_\mathrm{h} > 0$, $Z_0 > 0$, $B > N$, and $Z_\mathrm{min} > 0$.

Here, N_h represents the half-saturation constant, i.e., the number of individuals required to reach half the maximum biomass growth rate r_b. The variable $B(t)$ is constrained to values higher than the minimal possible total biomass, defined as the biomass of a single seed multiplied by the number of individuals $N(t)$. For the sake of simplicity and without loss of generality, we set $Z_\mathrm{min} = 0$ in the calculations.

This formulation results in two key dynamic interactions. First, the average plant size $\frac{B(t)}{N(t)}$ sets a threshold to the population growth: if individuals are too small, recruitment is negative. Second, the Michaelis-Menten term converts population size $N(t)$ into biomass productivity potential, reflecting a saturating resource uptake curve. As $N(t)$ increases, the term approaches 1, indicating efficient resource exploitation. If $N(t) = 0$, biomass cannot grow; conversely, $N_\mathrm{h} = 0$ implies that even a single individual could access all resources, which is an unrealistic scenario. This mechanism is visually summarised in Figure 1.

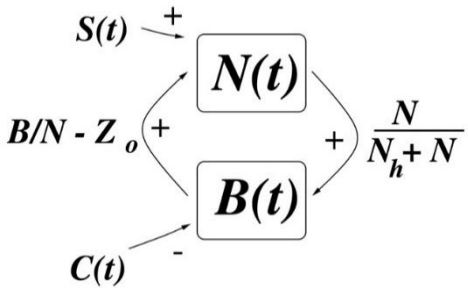

Figure 1. Diagram of the model. The two state variables, the number of individuals (box N) and the total biomass (Box B), are connected by two differential equations. Biomass influences the number of individuals via a function of the biomass/individuals ratio (or average individual size). The number of individuals influences biomass via the efficiency of capturing resources mediated by parameter N_h. Both functions result in a positive feedback loop between N and B, which is limited only by density-dependent effects on B. Additionally, seeding is represented by a function $S(t)$, which increases the number of individuals, and $C(t)$, which represents the biomass removed per unit of time. In the case of species where the distinction of individuals is not clear, because they grow horizontally and reproduce asexually, vegetation cover can take the place of the number of individuals in the model.

2.1.2. Biomass consumption

Populations of species living in productive ecosystems are (at least partially) subject to extraction. Biomass extraction is usually described through two different approaches. The first, proposed by Schaeffer [34], consists of a logistic population growth equation modified by a constant extraction term, typically denoted as C. This term can represent a fixed amount of biomass removed per time unit (independently of the population size) or a fixed proportion of the current biomass, as in Holling's type-I functional response. The second approach, pioneered by Noy-Meir [12], includes functional response curves that describe how extraction rates depend on resource availability, allowing more realistic nonlinear dynamics. In this study, we refer to models following the first approach as "Schaeffer-type", and to those using the second as "Noy-Meir-type" models.

Extraction can be direct (e.g., as in fisheries, where individuals are removed for consumption) or indirect, as in rangelands subject to extensive grazing, where livestock and wild herbivores consume vegetation. To distinguish these two processes (livestock and wild herbivory), we define:

- $L(t)$ as the biomass removed due to livestock grazing, and
- $H(t)$ as the biomass consumed by wild herbivory.

We can also define the total extraction term as $C(t) = L(t) + H(t)$, assumed as non-negative.

Population dynamics with extraction are classically represented by a logistic model with a removal term [34]:

$$\frac{\mathrm{d}}{\mathrm{d}t} B(t) = r\, B(t) \left(1 - \frac{B(t)}{K_\mathrm{b}}\right) - C(t), \tag{4}$$

with $C(t) > 0$.

Following the same procedure as in equation (3), let us extend the model to include both population structure and biomass extraction. While equation (4) represents a basic logistic growth model with an added extraction term $C(t)$, we refine this formulation by integrating the effects of individual-based growth and external biomass removal. This leads to a more complete and more realistic model of vegetation dynamics, as presented below:

$$\begin{aligned}\frac{\mathrm{d}}{\mathrm{d}t}B(t) &= r_{\mathrm{b}}\left(\frac{N(t)}{N_{\mathrm{h}} + N(t)}\right)B(t)\left(1-\frac{B(t)}{K_{\mathrm{b}}}\right) - L(t) \\ &\quad - H(t) \\ \frac{\mathrm{d}}{\mathrm{d}t}N(t) &= r_{\mathrm{n}}\left(\frac{B(t)}{N(t)} - Z_0\right)N(t) + S(t),\end{aligned} \tag{5}$$

with:

- $L(t) \geq 0$: biomass extracted by livestock,
- $H(t) \geq 0$: biomass consumed by wildlife,
- $S(t) \geq 0$: number of new individuals added through sowing or seedling planting.

We assume that the individuals added through the seeding term $S(t)$ have negligible biomass compared to adult individuals. While seeds and seedlings do carry some mass, their contribution to total biomass is orders of magnitude smaller than that of mature plants. Therefore, we approximate their initial biomass as zero. This simplification allows the model to remain analytically tractable while preserving the essential dynamics of early recruitment. As the introduced individuals grow, their contribution to biomass is dynamically incorporated via the feedback between $B(t)$ and $N(t)$.

2.1.3. Noy-Meir Model

Model (5) can be further improved by considering the equation, which considers extraction either as a constant value, or proportional to the plant population size ([12]). The extraction rate is represented by a functional response equation that describes the plant abundance per livestock animal, so that the term $C(t)$ becomes in turn a function of B, namely $C(t, B)$.

To study the behaviour of model (5) coupled with Noy-Meir's approach, we choose the Holling functional response models. Among the models of functional response available in the literature, Holling's curves are well-known and extensively studied by theoretical ecologists. Accordingly, extraction rate models become special cases of Holling's curves: an example at hand is the Schaeffer model, which usually describes the rate of extraction as a constant proportion of the population: $C(B) = c\,B(t)$. This formulation is similar to Holling's type-I functional response, under the aforementioned conditions.

Noy-Meir's models of seasonal grazing ([13], [14]), also recalled by Ungar [29], are an additional case of change in the use of resources. As a consequence, they can be reduced as a sigmoidal-type functional response III or to the generalised form proposed by Real [35]. Moreover, given a plant population size B_0, removal becomes zero because livestock may be removed or supplemented with balanced forage. Although the type-III functional response is usually related to prey switching, its structure is close to Noy-Meir's model. Animals switch food diet from natural pasture to other sources, as cattle under B_0 are supplemented with additional feed or are moved to different areas. Similar simple approaches to describe pasture consumption were already reported by Dieguez Cameroni & Fort [16].

Through a more general formulation, Holling's functional responses can be unified into a single equation. Extraction can thus be described by the generalised functional response proposed by Real [35], which extends Holling's approach through a shape exponent. This formulation is mathematically analogous to the enzyme kinetics model of Barcroft and Hill [36], a generalisation of the classical Michaelis–Menten equation for enzymes with multiple binding sites:

$$C(B) = N\frac{a\,B^c}{1 + a\,h\,B^c}, \tag{6}$$

with $c \geq 0$.

In equation (6), a is the herbivore encounter rate (efficiency), h is the handling time, N is the number of herbivores, and c is a curvature parameter that shapes the response. According to Real [35], c reflects the number of matches a predator should have with a prey before reaching full feeding efficiency (e.g., through learning). Alternatively, van Leeuwen et al. [37] considered c as the number of alternative prey types that drive changes in behaviour.

This flexible formulation replaces multiple classical responses: when $c = 0$, the extraction rate becomes constant and independent of biomass; for $c = 1$, it reduces to Holling's type II functional response; and for $c > 1$, it produces a sigmoidal (type III) response. As c increases, the transition becomes sharper, catching more abrupt changes in herbivore feeding behaviour than simpler models (e.g., Noy-Meir [14]).

Moreover, for $c > 1$, the functional response shows a well-defined inflection point, corresponding to the value of biomass B_0 at which the extraction rate increases most rapidly (i.e., where the derivative $\frac{\mathrm{d}}{\mathrm{d}B}C(B)$ reaches its maximum). This point can be interpreted as the threshold biomass level required to trigger a switch in foraging intensity.

The inflection points B_0, defined as the biomass level at which the extraction rate increases most rapidly, can be derived analytically by finding the maximum of the first derivative of equation (6). For $c > 1$, the inflection point is given by:

$$B_0 = \left(\frac{c-1}{a\,h\,N\,(c+1)}\right)^{1/c}. \tag{7}$$

This expression shows that the position of the threshold depends not only on the curvature parameter c, but also on the number of herbivores N, their efficiency a, and the handling time h. As c increases, B_0 shifts to higher biomass values and the transition becomes steeper. This property allows the model to describe switching behaviour more realistically in systems where foragers adjust their feeding intensity in response to changing prey or plant abundances.

2.2. Analysis

The behaviour of model (5) was analysed from an analytical and numerical standpoint. The analytical part focused on the research of nontrivial equilibrium points (i.e., a combination of parameters so that the growth rate is zero), while numerical simulations were more prone to study the parameter variation sensitivity and its effect on stable or non-stable equilibrium points.

As stated in the previous sections, model (5) is an extension of Schaeffer's [34] and Noy-Meir's [12] equations, which are, in turn, an extension of the logistic growth. According to these properties, we first wondered if model (5) conserved the well-

Table 1. Default parameter values used in the numerical simulations. The first column lists the parameter names as they appear in equations (1)–(6). The second column shows the default values used in simulations, and the third column indicates the parameter ranges applied in the Sobol sensitivity analysis following Saltelli's sampling scheme.

Parameter	Default value	Sobon Range	
		min	max
$N_{t=0}$	1.0	0.0	10.0
$B_{t=0}$	1.0	0.0	10.0
r_n	0.1	0.0	1.0
r_b	0.1	0.0	1.0
Z_0	1.0	0.0	1.0
K_b	10.0	0.0	10.0
N_h	0.0	0.0	1.0
N_i	0.0	0.0	1.0
L	0.0	-	-
H	0.0	-	-
$C(L+H)$	0.0	0.0	1.0
h	0.0	0.0	1.0
a	0.5	0.0	1.0
c	1.0	0.0	4.0

known equilibrium points of the logistical model with extraction, and which was the effect of the additional parameters introduced with our formulation. We also carried out a global sensitivity analysis of the model using the Sobol methods. The analysis was carried out testing the sensitivity of variables and initial conditions.

Numerical analyses were carried out by fixing the initial conditions and solving the model by considering different combinations of parameters. Extinction, increase, or decrease in the state variables was considered for large time ranges to achieve the goal of this part of the study.

For the sake of simplicity, the analyses were carried out under constant environmental conditions, namely that the parameters r and K were not modified by external factors. Unless stated otherwise, the default parameters and initial conditions were set as listed in Table 1.

2.2.1. Global sensitivity analysis

To evaluate the model's sensitivity to variations in parameters and initial conditions, we conducted a global sensitivity analysis (GSA) using the Sobol variance decomposition method. This approach captures both first-order effects (individual parameter contributions) and total effects (including interactions), making it well-suited for nonlinear ecological systems.

Due to computational constraints, we replaced a single large Sobol run with multiple smaller, independent runs. Each iteration used 1,024 parameter sets generated via Saltelli's sampling scheme, covering 14 model parameters and initial conditions. This approach, repeated over 64 to 128 iterations, allowed a more robust estimation of sensitivity indices by reporting the median and 2.5–97.5 % quantile range across runs, thereby reducing numerical artifacts and accounting for stochastic variability. The analysis focused on the final total biomass value from each simulation, which reflects long-term system behaviour. Water availability was treated as auxiliary and excluded from the sensitivity metrics.

Simulations that led to trivial dynamics (e.g., full extinction) were excluded to ensure sensitivity estimates were conditioned on ecologically viable outcomes. This filtering avoided bias from boundary behaviours and highlighted parameter effects within the meaningful dynamic range of the system. Sobol indices were computed using the SALib Python library. Both first-order and total-effect indices were used to rank parameter influence and identify key drivers of vegetation dynamics. Additional iterations are being processed to refine these estimates.

2.2.2. Analysis without extraction

To observe the effect of different initial conditions N_0 and B_0 on the system dynamics, and the interaction between N and B under different combinations of N_h, Z_0, and S, we analysed the model behaviour without extraction. The analysis was carried out following three steps:

1) Interaction of N and B at different values of N_h. In the first step, we kept Z_0 and S constant, varying only N_h to observe its behaviour on the long-term dynamics of the model. As N_h affects the efficiency in obtaining the resources, it was the first to be analysed.
2) Interaction of N and B at different values of N_h and Z_0. We added different values of Z_0 to the variation in N_h. With this analysis, we observed the interaction between the efficiency in obtaining resources as a function of the number of individuals and the optimum average size of the individuals.
3) Effect of the constant seedling. We studied the effect of the continuous addition of a constant number of new individuals (either via seeding or seedling), but not biomass, on the population dynamics. As the model differentiates individuals from biomass, it is worth studying the effect of artificially increasing the plant population on an extensive system, while keeping the biomass constant. For the sake of simplicity, seeding was also assumed constant and continuous.

2.2.3. Analysis with constant extraction

We repeated the sequence of analyses in Section 2.2.1 considering extraction as well. As previously stated, we considered as a starting point the well-known equilibrium points of logistic models with extraction. Then, we investigated the variations in the system's stability if the population state variables were split into biomass and number of individuals. The following sequence was carried out:

1) Recruitment (derivative) at different levels of N, B and N_h: We analysed how the stability of the logistic model with extraction can be affected by the separation of biomass and the number of individuals. This analysis was focused on the derivative of the model from equation (5) under extraction conditions.
2) Effect of extraction at different N_h values (time series): here we studied the interaction between N_h and C using the simulations of different values of both variables.
3) Effect of extraction at different Z_0 at $N_h > 0$ (time series): we analysed the interaction between Z_0 and C under different combinations of values, always considering $N_h > 0$.
4) Effect of extraction with seedling at $N_h > 0$ (time series): we analysed the interaction between Z_0, S and C under different combinations of values, always with $N_h > 0$.

2.2.4. Analysis with functional response extraction

The same analysis as in Sections 2.2.1 and 2.2.2 was carried out on the model considering Holling's type-II functional response model (7), with $c = 1$ to see the effect of Noy-Meir's saturation curve on extraction. According to this model, the extraction decreases when the biomass is low.

2.3. Numerical methods

The same combination of parameters as described in the previous sections was considered to carry out a series of numerical simulations. A simulation consisting of 120 time units representing plant generation time, at 1/1000 time steps integrated via the Runge-Kutta 4 (RK4) method was carried out for each combination of parameters. Numerical analyses were carried out through an *ad hoc* Python 3.10 scripts including the NumPy library version 1.21.5 [38]. The code to fully reproduce the results of this study is publicly available at [39].

Default and range of parameters used in the simulation are listed in Table 1. Unless stated explicitly, these parameters are used in the simulations as well, to see if parameter values are within the interval of parameters used in the Sobol Global sensitivity analysis.

3. RESULTS

3.1. Global sensitivity analysis

The results of the Sobol sensitivity analysis are presented in Figure 2 for the *biomass* variable and in Figure 3 for the *number of individuals*. In both cases, sensitivity to initial conditions ($B = 0$, $N = 0$) was not significant, as the 95 % confidence intervals of the Sobol indices included zero, indicating that any effect was within the range of numerical error (Figure 2a and b).

First-order Sobol indices were significant for the parameters r_n, r_b, Z_0, K_b, S_i, and C (Figure 2a). Second-order effects were significant for all parameter pairs, except those involving initial conditions (Figure 2b). No significant interactions between parameters were observed beyond second-order effects (Figure 2c).

The most influential parameter for *biomass* was Z_0, accounting for over 40 % of the total variance. The second most important was r_n, contributing approximately 15 %, followed by K_b, S_i, r_b, and C. All remaining parameters accounted for less than 5 % of the total variance and were therefore considered comparatively unimportant (Figure 2a). Significant positive second order interactions were observed between r_n, and K_b (Figure 2c).

The most influential parameters in the case of the *number of individuals* were r_b, K_b, and c, the shape parameter of the herbivores' functional response. Other significant variables (i.e., C, a, and h, in order of importance) were not significant in terms of first-order effects (Figure 3a). As with *biomass*, total-order coefficients were significant for all model parameters but not for the initial conditions (Figure 3b). No significant positive second order interactions were observed (Figure 3c).

3.2. Analysis under no extraction

3.2.1. Equilibrium points

Equation (3) tends to equilibrium with respect to biomass when $\frac{\mathrm{d}}{\mathrm{d}t}B(t) = 0$, as in the logistic equation. The biomass term from this equation is effectively separated from the number of individuals if $N_\mathrm{h} = 0$ and collapses into a logistic model with no influence of the number of individuals on biomass. Accordingly, it reaches a nontrivial equilibrium when $B = K$, while the number of individuals slowly converges to $N = \frac{B}{Z_0}$. When $N_\mathrm{h} > 0$, the two equations are connected, but only N affects the absolute value of r, since the term $\frac{N}{N_\mathrm{h}+N}$ can only be positive. The equilibrium point is the same: the biomass equation is more stable at higher values of N, since its derivative is higher as B approaches K. As above, N also tends to $\frac{B}{Z_0}$.

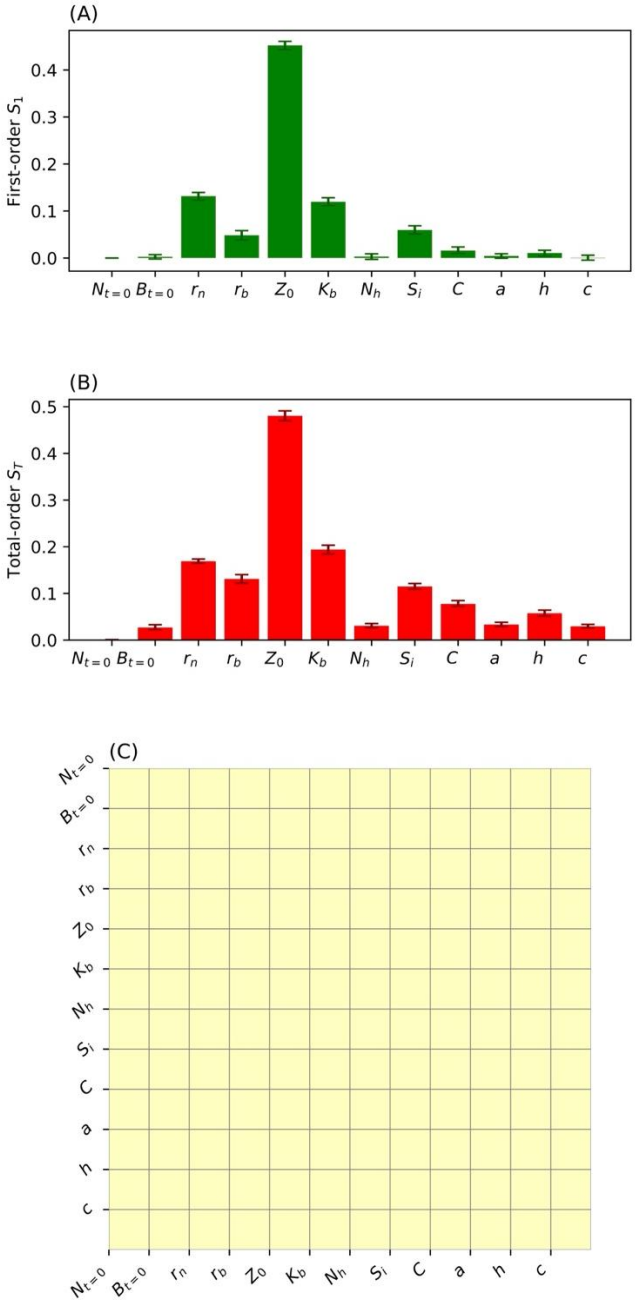

Figure 2. Global sensitivity analysis of the biomass state variable (B) with respect to model parameters and initial conditions. Panel (A) shows the first-order Sobol indices, panel (B) displays the second-order indices, and panel (C) presents the total-interaction indices. Error bars represent the 95 % quantile ranges based on 128 independent runs of the Sobol analysis, with bars indicating the median values. In panel (C), non-significant indices (those whose 95 % quantile range includes zero) are shown in yellow, while significant indices are shown in blue.

Including the effect of seedlings, the equilibrium is reached only if no seeds or seedlings are introduced into the ecosystem, as $S(t)$ is restricted to be positive. Otherwise, it compensates for an increase in population size, leading to $r_\mathrm{n}\left(\frac{B}{N} - Z_0\right)N = S(t)$ for $\frac{B}{N} > 0$, while if $S(t) = 0$, the equilibrium point is $\frac{B}{N} = Z_0$. The system (3) reaches equilibrium when both $\mathrm{d}N$ and $\mathrm{d}B$ are

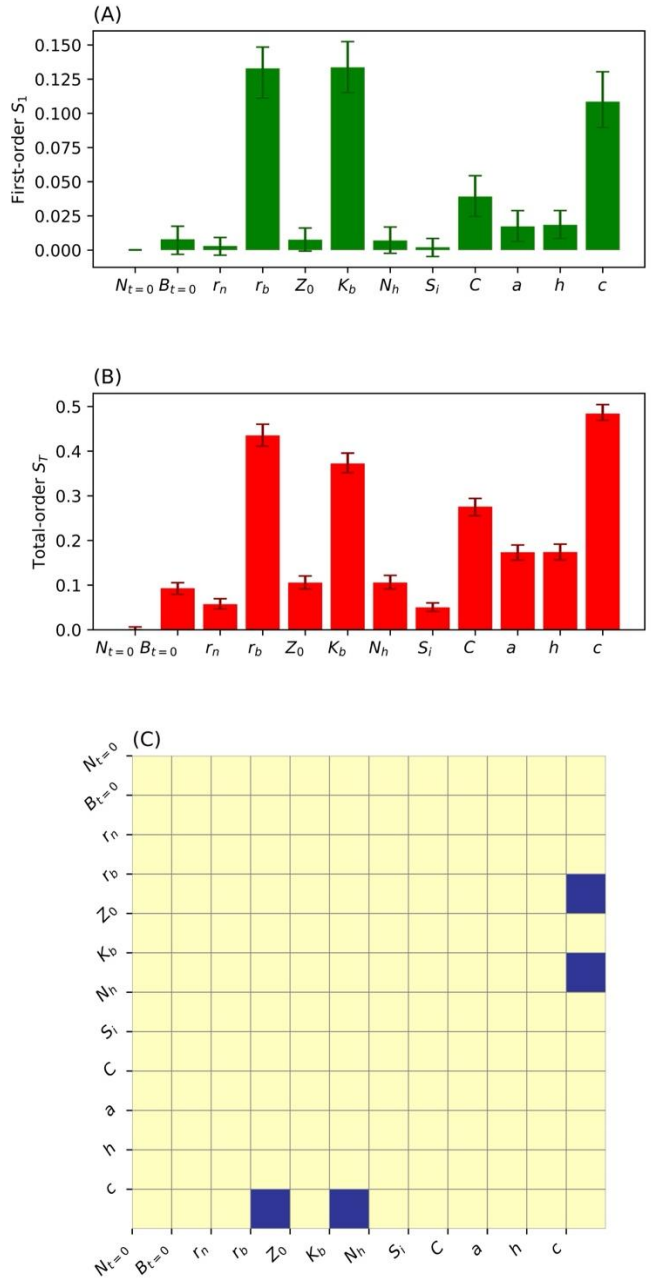

Figure 3. Global sensitivity analysis of the number of individuals N state variable with respect to model parameters and initial conditions. Panels (A), (B), and (C) display the first-order, second-order, and total-interaction Sobol indices, respectively. Blue bars in panel (C) indicate significant indices (95 % quantile range does not include zero), while yellow bars denote non-significant ones. Error bars represent 95 % quantiles across 128 Sobol runs, with central bars showing the median values.

zero, so the conditions $B = K_\mathrm{b}$, and $\frac{B}{N} = Z_0$ or $r_\mathrm{n}\left(\frac{B}{N} - Z_0\right)N = S(t)$ should occur simultaneously.

The Jacobian matrix of the system at equilibrium is considering the autonomous case with $S(t) = 0$ (no seeding), where the equilibrium point is given by $B^* = K_\mathrm{b}$ and $N^* = \frac{B^*}{Z_0}$. The evaluation of the Jacobian at this point yields two eigenvalues (see appendix for the complete analysis): one associated with biomass dynamics and another with the number of individuals. The biomass-related eigenvalue is negative for $N > 0$, reflecting logistic-like local stability. The eigenvalue associated with N is $\lambda = r_\mathrm{n}\,(1 - Z_0)$, which is negative if $Z_0 > 1$, indicating stability, and positive otherwise, indicating local instability. Thus, the nontrivial equilibrium is locally stable when the per capita biomass requirement Z_0 exceeds one, reflecting a density threshold for persistence.

3.2.2. Vegetation dynamics

Figure 4 shows the effects on N and B at different values of N_h. When $N_\mathrm{h} = 0$, even a single plant can obtain all resources. The number of individuals converges over time regardless of the initial conditions $\frac{K}{Z_0}$. As in Section 3.1.1, K was set to 10 and $Z_0 = 1$, so that $\frac{K}{Z_0} = 10$. When the average biomass of the individuals was lower than Z_0, the population trend was initially downward and then increased to reach the same asymptotic value observed in the other simulations (Figure 4A). In all cases, biomass approached K sigmoidally, maintaining the same rate that depends only on initial conditions (Figure 4B). The average biomass approached Z_0 with a sharp decrease at higher values, an increase when the average initial biomass was equal to Z_0, and an overshoot when the initial biomass was lower than the equilibrium value. The average biomass converged towards Z_0 at the end of the simulations (Figure 4C).

If $N_\mathrm{h} = 1$, the biomass is connected to N, and the population dynamics change accordingly, as shown in Figure 4D. The number of individuals increased sigmoidally if the initial biomass was $B_0 = 1$; but for low values, the population increased too

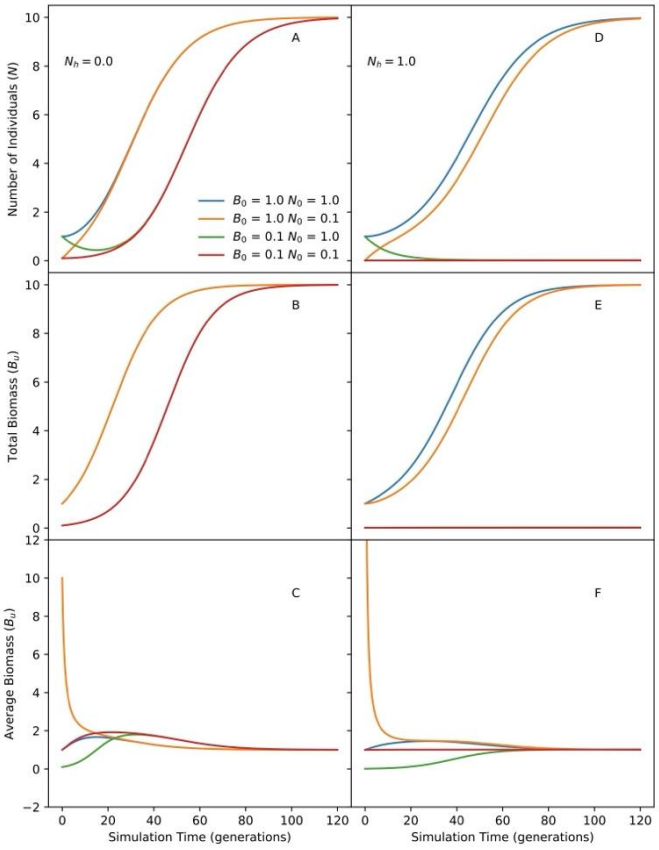

Figure 4. Population dynamics according to the model (3) with different initial conditions in terms of N_0 and B_0, with $N_\mathrm{h} = 0$ (left column) and $N_\mathrm{h} = 1$ (right column). The upper row of plots is the number of individuals as a function of time; the second one is biomass; and the third one is the average individual size. N_0 and B_0 are the initial conditions of the state variables N and B, each combination of the initial conditions is represented with different line colours as shown in the caption of plot A. Simulation time unit is in plant generations.

slowly and maintained a low value over the whole simulation time. Considering the combination $B_0 = 0.1$ and $N_0 = 1$, the population decreased until approaching the same asymptotic values observed for the combination $B_0 = 0.1$ and $N_0 = 0.1$. With an initial population of $N_0 = 1$ and higher initial conditions, the population grew faster than with $N_0 = 0.1$, even though the initial biomass was the same, reflecting a higher efficiency in capturing the resources caused by more initial individuals. In Figure 4E, the pattern is similar: with low initial biomass, the population grew too slowly to appreciate a noticeable difference in the plot, whereas the population with a higher initial number of individuals grew faster in terms of biomass. In Figure 4F, all populations converged rapidly into an average individual size of $\frac{B}{N} = Z_0$, with one case ($B_0 = 1$ and $N_0 = 1$) growing to average sizes higher than Z_0, and then declining to that value.

3.2.3. The influence of seeding

Repeating the analysis from Section 3.1.2, but now with seeding, yields different results. In both cases, the population reached an asymptotic value of 12, which is above the expected $\frac{K}{Z_0} = 10$, due to the continued addition of individuals, resulting in higher N. When $N_\mathrm{h} = 0$, there is no difference in biomass dynamics (Figure 5B is similar to Figure 4B), but the number of individuals grows faster (Figure 5A), because they are continuously introduced, leading to their smaller average size (Figure 5C). The reason is that seeds are the smallest possible individuals and are averaged with the rest of the population. When $N_\mathrm{h} > 0$ with seeding, the population becomes more efficient in acquiring resources and therefore grows faster in terms of the number of individuals and biomass (Figure 5A and B). However, the average individual size remains smaller (Figure 5C) than when no seeding occurs (Figure 5C).

3.3. Analysis under constant extraction

3.3.1. Equilibrium points

Model (5) approaches equilibrium (in terms of biomass) if $\frac{\mathrm{d}}{\mathrm{d}t} B(t) = 0$. Accordingly, when the extraction $C(t) = L(t) + H(t)$ is greater than zero, it follows:

$$r_\mathrm{b} \left(\frac{N}{r_\mathrm{h} + N}\right) B \left(1 - \frac{B}{K_\mathrm{b}}\right) = L(t) + H(t) = C(t). \tag{8}$$

Accordingly, without extraction ($C = 0$), biomass does not change when its carrying capacity ($B = K_\mathrm{b}$) is already reached. If $C(t) > 0$, the equilibrium point is similar to the Schaeffer model, namely $\mathrm{d}B = C(t)$. As in the section above, if $N_\mathrm{h} = 0$, the model (7) becomes a simple logistic equation for biomass, thus extraction can be reduced to the Schaeffer model. By increasing N_h, the system becomes less efficient, as the individual plants cannot reach all the system resources. The effect of increasing N_h on the system is shown in Figure 6A–C. As N_h increases, the derivative becomes lower, and the biomass extracted from the ecosystem decreases proportionally. On the other hand, as N increases, the population becomes more efficient and compensates for the effect of increasing N_h, so the derivatives become more closely packed, as it is possible to observe by comparing Figure 6C and Figure 6A.

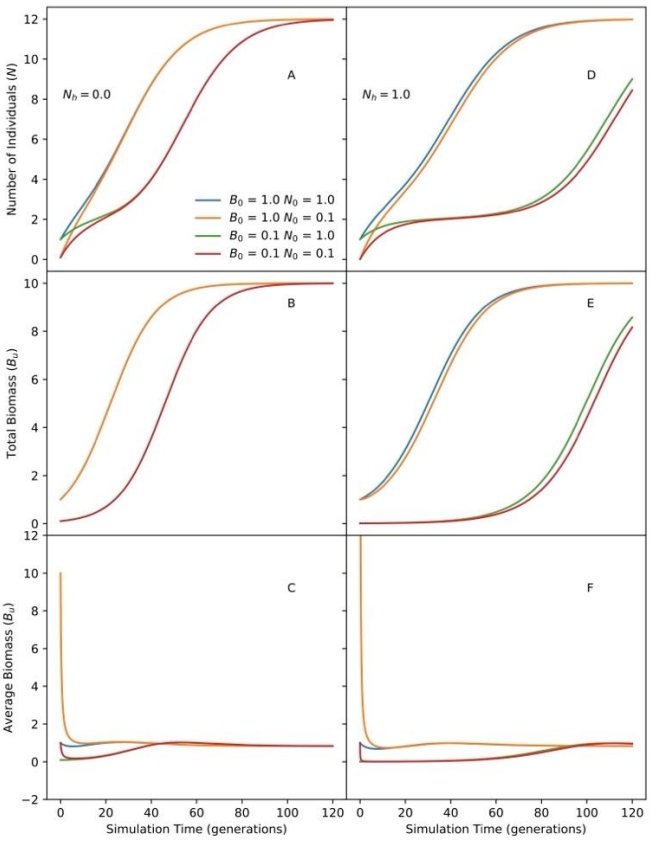

Figure 5. Population dynamics according to the model of equation (3) with seeding under different initial conditions in terms of N_0 and Z_0, with $N_\mathrm{h} = 0$ (left column) and $N_\mathrm{h} = 1$ (right column). The references are the same as in Figure 4. Simulation time unit is in plant generations.

3.3.2. Maximum biomass extraction

The model has many similarities with most logistic models with extraction. Let us define $\mathrm{d}B_\mathrm{max}$ as the maximum derivative of the biomass function and B_x as the value of the variable in which $\mathrm{d}B_\mathrm{max}$ occurs. Moreover, $\mathrm{d}B_\mathrm{min}$ indicates the minimum derivative of B at which the system is sustainable, and B_min is the value of B at which $\mathrm{d}B_\mathrm{min}$ occurs. The values at which B_min and $\mathrm{d}B_\mathrm{min}$ occur are depicted with red lines in Figure 6. If $C(t) = 0$, the nontrivial equilibrium points are locally stable. When $C(t) < \mathrm{d}B_\mathrm{max}$, the system becomes bistable. If $C(t) = dB_\mathrm{max}$, the system has an equilibrium point at $B = B_\mathrm{x}$, but if $B < B_\mathrm{x}$, the system approaches zero. When $C(t) < \mathrm{d}B_\mathrm{max}$, the system has a stable equilibrium point if $\mathrm{d}B = C(t)$ and $B > B_\mathrm{min}$ (blue lines in Figure 6), and an unstable equilibrium point if $\mathrm{d}B = C(t)$ and $B < B_\mathrm{min}$ (red lines in Figure 6). For B values lower than the red line of Figure 6, the system approaches zero. The main difference with any simple logistic model is that B_x is not $K_\mathrm{b}/2$, but it is also dependent on N.

$\mathrm{d}B_\mathrm{max}$ is equal to

$$\mathrm{d}B_\mathrm{max} = \frac{r_\mathrm{b}\, N}{N_\mathrm{h} + N} K_\mathrm{B} \left(1 - \frac{\frac{K_\mathrm{B}}{2}}{K_\mathrm{B}}\right) \tag{9}$$

that can be rewritten as:

$$\mathrm{d}B_\mathrm{max} = r_\mathrm{b}\, K_\mathrm{B} \frac{N}{2(N_\mathrm{h} + N)}. \tag{10}$$

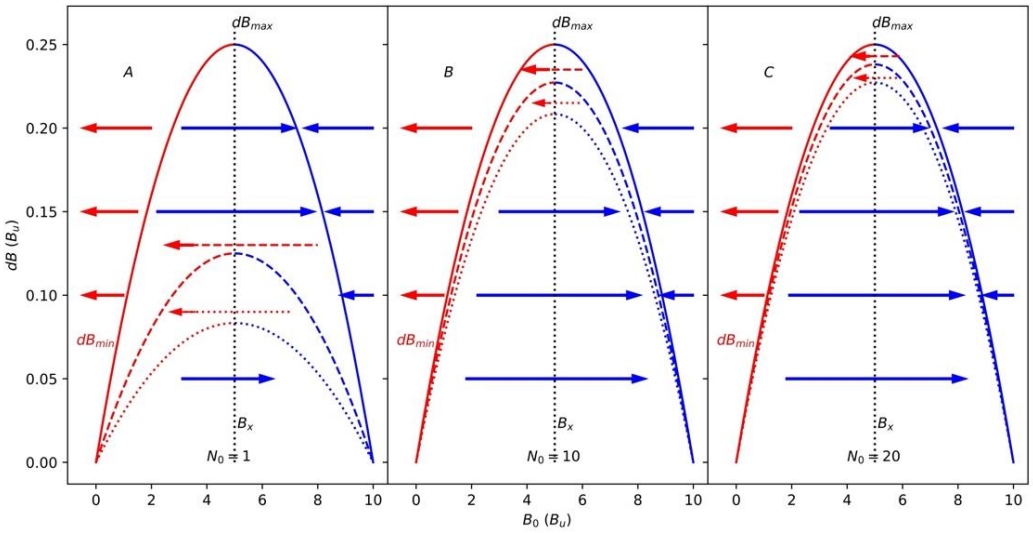

Figure 6. Derivative of B under different initial conditions of N_0 and B_0. Solid lines are with $N_\mathrm{h} = 0$, dashed with $N_\mathrm{h} = 1$, and dotted with $N_\mathrm{h} = 2$. In contrast, different plots show the derivative or the population at other initial conditions, being $N_0 = 1$ for Plot A (left), $N_0 = 10$ (Plot B, centre), and finally $N_0 = 20$ (Plot C, right). Red lines indicate unstable equilibrium, and blue lines indicate stable equilibrium. The values of dB and B at the red lines are called $\mathrm{d}B_{\min}$ and $B_{\min}$, respectively. Red arrows indicate the population trend toward a population decrease or collapse for a given constant extraction rate, whereas blue lines indicate population trends towards stable equilibrium.

For sufficiently large N, the term $\frac{N}{2(N_\mathrm{h}+N)}$ is close to $N/2$, so it becomes indistinguishable from the logistic with $\mathrm{d}B_{\max} = r_\mathrm{b}\frac{K_\mathrm{B}}{2}$. Therefore, the maximum extraction rate possible for a given population depends not only on biomass but also on the number of individuals and on their efficiency in consuming resources. As more individuals are needed to consume half of the resources of the system, the population is less efficient. Thus, $\mathrm{d}B_{\max}$ decreases accordingly with N_h, approaching zero as it increases (Figure 7A). With more individuals the population becomes more efficient, leading to an increase toward $r\frac{K_\mathrm{b}}{2}$ proportionally to N (Figure 7B).

If $\mathrm{d}B_{\max} > \big(L(t) + H(t)\big)$, it is possible to have a stable system with extraction. In this case, the critical point is when $\mathrm{d}B$ is just enough to allow the extraction of $(L + H)$ biomass. Then, the unstable lower equilibrium points from the logistic with extraction can be obtained considering the Michaelis–Menten curve from N multiplying $4\,K\,C$:

$$\mathrm{d}B = \frac{K \pm \sqrt{K^2 - 4\,K\,C\left(\frac{N}{r_\mathrm{h}+N}\right)r^{-1}}}{2}. \tag{11}$$

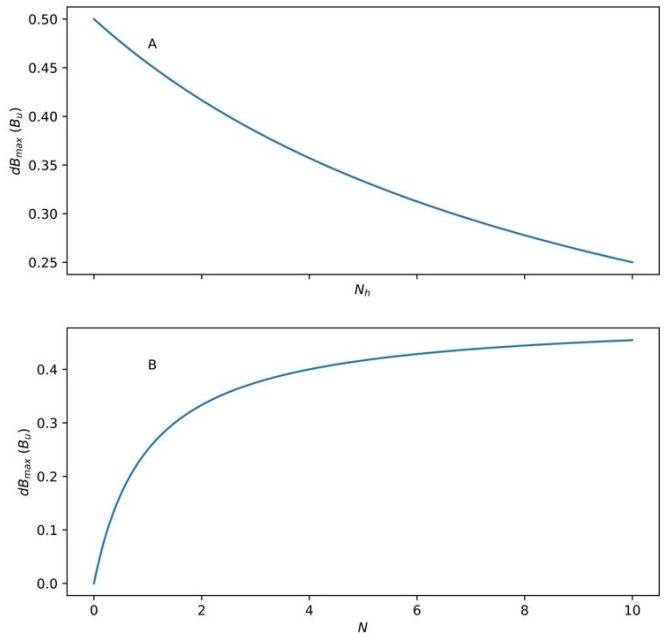

Figure 7. Maximum sustainable extraction rate $\mathrm{d}B_{\max}$ for a plant population as a function of N_h (above) with $N_0 = 10$, and as a function of N_0 with $N_h = 1$ (below).

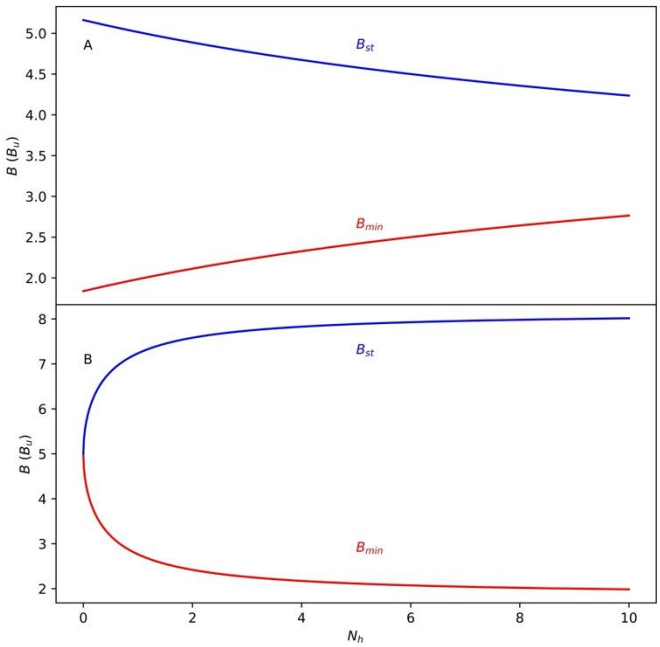

Figure 8. Minimum and maximum B of stable equilibrium ($B_{\min}$) as a function of N_h (Plot A, above) with $N_0 = 10$, and N_0 with $N_\mathrm{h} = 1$ (Plot B, below) under a constant extraction rate of $C = 0.1$. Blue lines indicate the value of B at which the stable equilibrium occurs (B_{st}), and red lines the value of B at which the minimum sustainable rate occurs ($B_{\min}$).

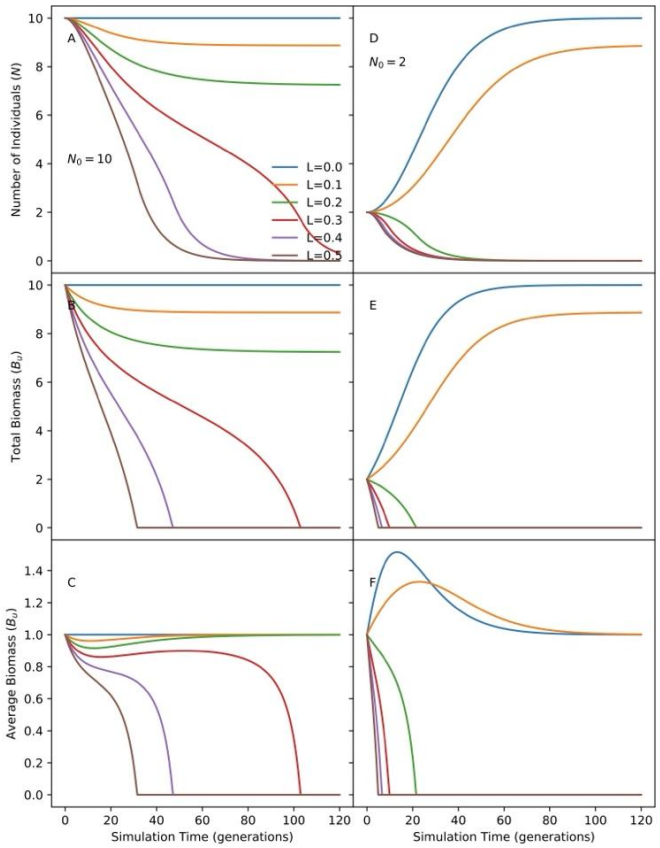

Figure 9. The effect of initial conditions on the long-term dynamics of the vegetation model under different extraction rates by livestock L. As in Figure 4, the plot shows the number of individuals, total biomass, and average biomass as a function of time with different levels of extraction, plots on the left column are with $N_0 = 10$ (on the carrying capacity). On the right column with $N_0 = 2$ (below $B_{\max}$), L ranged from zero to 0.5 (the maximum possible extraction rate, according to equation (6), was 0.25), and other parameters were $K = 10$, $r = 0.1$, $N_h = 0$, and $S = 0$.

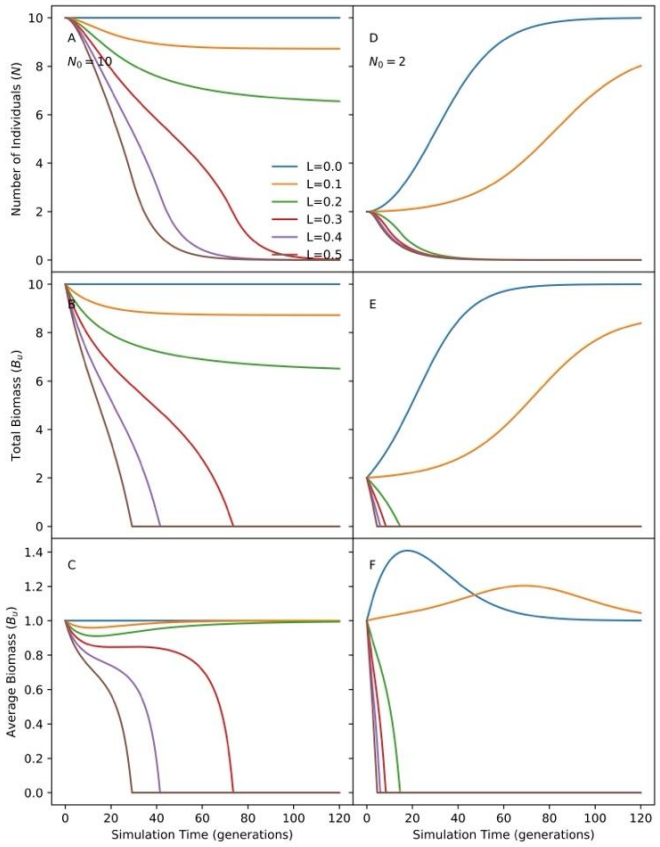

Figure 10. The effect of the initial conditions on the long-term dynamics of the vegetation model under different extraction rates by livestock L, as in Figure 9, but now with $N_h = 1$. As in Figure 4 and 9, the plot shows the number of individuals, total biomass, and average biomass as a function of time with different levels of extraction; plots on the left column are with $N_0 = 10$ (on the carrying capacity). On the right column with $N_0 = 2$ (below $B_{\max}$), L ranged from zero to 0.5 (the maximum possible sustainable extraction rate, according to equation (6), was 0.25), and other parameters were $K = 10$, $r = 0.1$, and $S = 0$.

Consequently, the term narrows the interval of stability (the difference between $B_{\min}$ and B_{st}), decreasing with N_h (Figure 8B), and increases with C (Figure 8B). Therefore, a system that needs more N to consume more efficiently the resource is more sensitive to biomass extraction.

3.3.3. The effect of extraction at different N_h values (time series)

The population with extraction rates higher than $dB_{\max}$ collapsed, regardless of the initial conditions (brown and purple lines in Figure 9A, B, C; brown, purple, red, and green lines in Figure 9D, E, F). If the total biomass approaches zero (brown and purple lines in Figure 9B; brown, purple, red, and green lines in Figure 9E), the number of individuals decreases asymptotically to zero (brown and purple lines in Figure 9BA; brown, purple, red, and green lines in Figure 9D), reflecting steady constant mortality once the average size is below Z_0. With extraction rates lower than $dB_{\max}$, and initial conditions such that the population does not produce enough individuals to keep up with the extraction rate (the combination of population and dB are on the left of Figure 6), the population collapses as well (red and green lines in Figure 9E). In terms of biomass, the model (6) is, up to here, close to the Schaeffer equation as in the case of $N_h = 0$. The average size of the individuals for initial conditions of $N_0 = 10$ at first decreases and then becomes stable until the population collapses for $L > dB_{\max}$. Analogously, the average size of the individuals asymptotically increases to Z_0, with a lower extraction rate, while size recovery is faster (red, green, orange, and blue lines in Figure 9C). With lower N_0, the average size of the individuals at first increases above Z_0, and then asymptotically approaches Z_0 (orange and blue lines in Figure 9F). The process is faster for lower extraction rates, while with higher extraction rates the average size of the individuals is temporarily higher (orange and blue lines in Figure 9F). For substantially high extraction rates the population collapses, the average size of the individuals never reaches stability, and rapidly declines to zero (brown, purple, red, and green lines in Figure 9F).

3.3.4. The effect of extraction at different Z_0 at $N_h > 0$ (time series)

If N_h is greater than zero, the system becomes less efficient in acquiring the resources available in the ecosystem and the maximum rate of extraction becomes smaller (Figure 6), so that the population is more likely to collapse. When $N_h = 1$ (Figure 10), the system resembles the situation shown in Figure 9. In this case, the collapse is faster, both in terms of the number of individuals (Figure 10A, D) and of biomass (Figure 10B, E). The growth/recovery is slower as well (Figure 10D, E), and the pattern of variation on the average individual size from the plot in Figure 10F is a delayed version of the plot in Figure 9F for the extraction rates, where the population does not collapse.

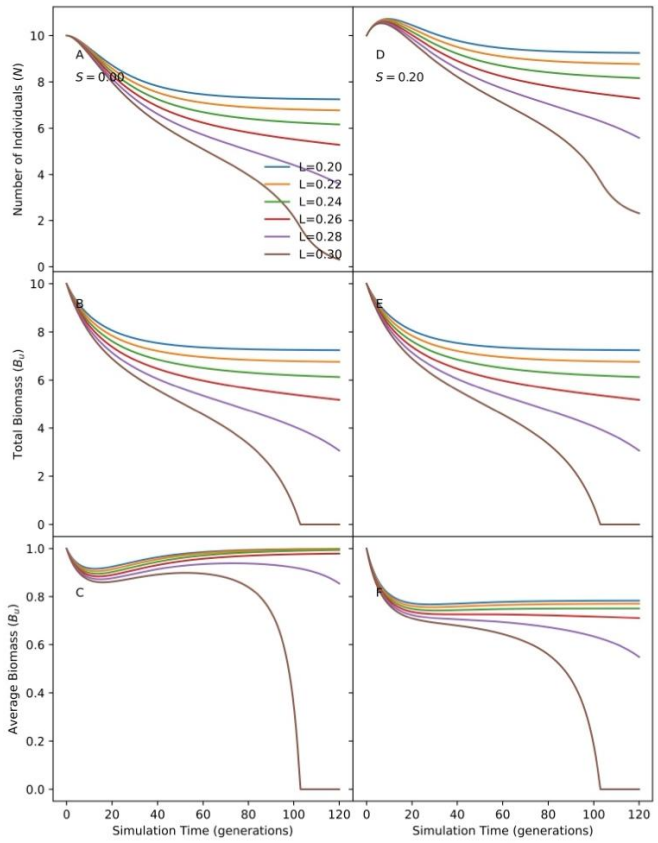

Figure 11. The effect of initial conditions on the long-term dynamics of the vegetation model under different extraction rates by livestock L, as in Figure 9, but now with different values of S. As in Figure 4, Figure 9, and Figure 10, the plot shows the number of individuals, total biomass, and average biomass as a function of time with different levels of extraction; plots on the left column are with $S = 0$ (no seeding) and on the right column with $S = 0.2$. L ranged from 0.2 to 0.3 (the maximum possible sustainable extraction rate, according to equation (6), was 0.25 for this combination of parameters), and other parameters were $K = 10$, $r = 0.1$, and $N_h = 0$.

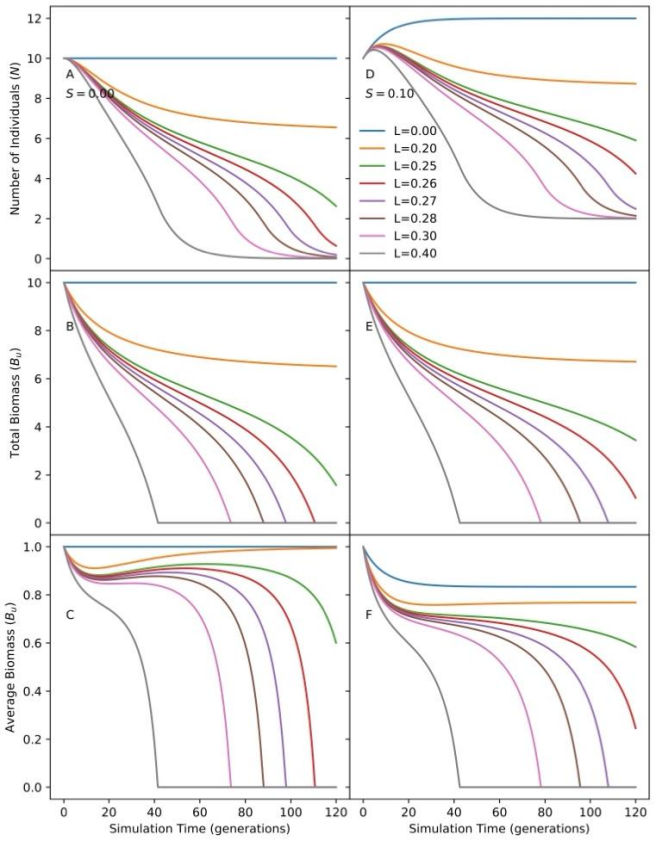

Figure 12. The effect of initial conditions on the long-term dynamics of the vegetation model under different extraction rates by livestock L, as in Figure 11, but now with $N_h = 1$. As in Figure 4, Figure 9, Figure 10, and Figure 11, the plot shows the number of individuals, total biomass, and average biomass as a function of time with different levels of extraction; plots on the left column are with $S = 0$ (no seeding) and on the right column with $S = 0.2$. L ranged from 0.2 to 0.3 (the maximum possible sustainable extraction rate, according to equation (6), was 0.25 for this combination of parameters), and other parameters were $K = 10$, $r = 0.1$, and $N_h = 1$.

3.3.5. The effect of extraction with seedling at $N_h > 0$ (time series)

Seeding does not affect dB_{max} directly, but the replenishing of size zero individuals increases the efficiency of the system, or rather, it decreases the rate at which the system loses efficiency due to continuous extraction. However, the system is dependent on N_h. If $N_h = 0$ (Figure 11A–D) adding seeding does not produce any effect, and the population collapses because the addition of individuals does not increase the system's efficiency. If $N_h > 0$, seeding influences the dynamics of the system, as N_h limits its efficiency delaying (and sometimes avoiding) the collapse under constant extraction rates (Figure 12A–D). The effect of seeding becomes stronger as N_h increases, because the addition of individuals increases, even more, the efficiency of the system, avoiding or delaying its collapse (Figure 13A–D).

3.4. Analysis under functional response extraction

The interaction between N_h, seeding, N_0, and the type of extraction (constant, type-I and type-II functional responses) is shown in Figure 14. Overall, as N_h increases, the curve decreases and, therefore, the system is more likely to collapse, and thus less sustainable (Figure 14A). With constant extraction, the system is less sustainable at lower population sizes in terms of biomass, and, with type-I and type-II functional responses, the system increases its sustainability. At lower biomass levels, the difference between curves with high and low N_h might make the difference between sustainable and unsustainable systems.

By increasing seeding, it is also possible to increase the sustainability of the system, as shown in Figure 14B, although its effect is much smaller because it causes low changes in the number of individuals per time unit. Figure 14C shows the effect of the different numbers of individuals at time $t = 0$, which is equivalent to the effect of massive seeding as well. The system increases its output at a higher N but, as in Figure 6A–C and Figure 7B, it saturates in a diminishing return way. Accordingly, higher N might increase the sustainability of the system, especially under low biomass conditions. Overall, sustainability is achieved if $dB(B) > C(B) = \frac{a_h B_c}{1+a_h B_c}$ for $B < B_{max}$.

4. DISCUSSION

4.1. Summary of the model

This study introduces a new model of plant population dynamics, a useful tool to understand vegetation dynamics in grazing contexts, where plant populations are used by extensive livestock systems. In particular, we considered farming systems where: *i)* the human intervention is limited to a pastoral practice, *ii)* only a limited amount of plants are introduced to increase the population (via seeding or seedlings), *iii)* this action has a small

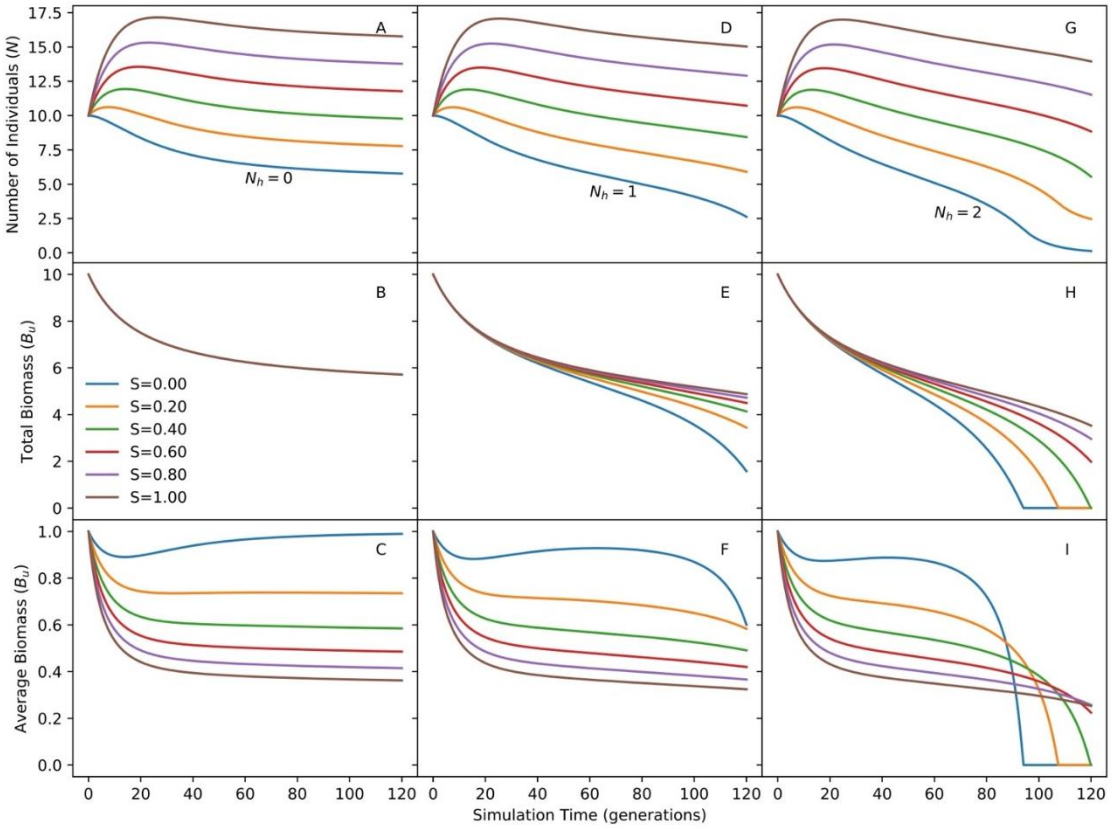

Figure 13. Interaction between seeding S and resource efficiency use N_{h} on the long-term population dynamics according to model (5), considering a constant extraction rate L of 0.25 (the maximum possible sustainable extraction rate, according to equation (5), was 0.25 for this combination of parameters and $N_{\mathrm{h}} = 0$). As in Figure 4, Figure 9, Figure 10, and Figure 11, the upper plot shows the number of individuals, in the middle the total biomass, and at the bottom the average biomass as a function of time. Different line colours show different seeding levels. Each column has a different value of resource efficiency use, with $N_{\mathrm{h}} = 0$ (left column), $N_{\mathrm{h}} = 1$ (central column), and $N_{\mathrm{h}} = 2$ (right column).

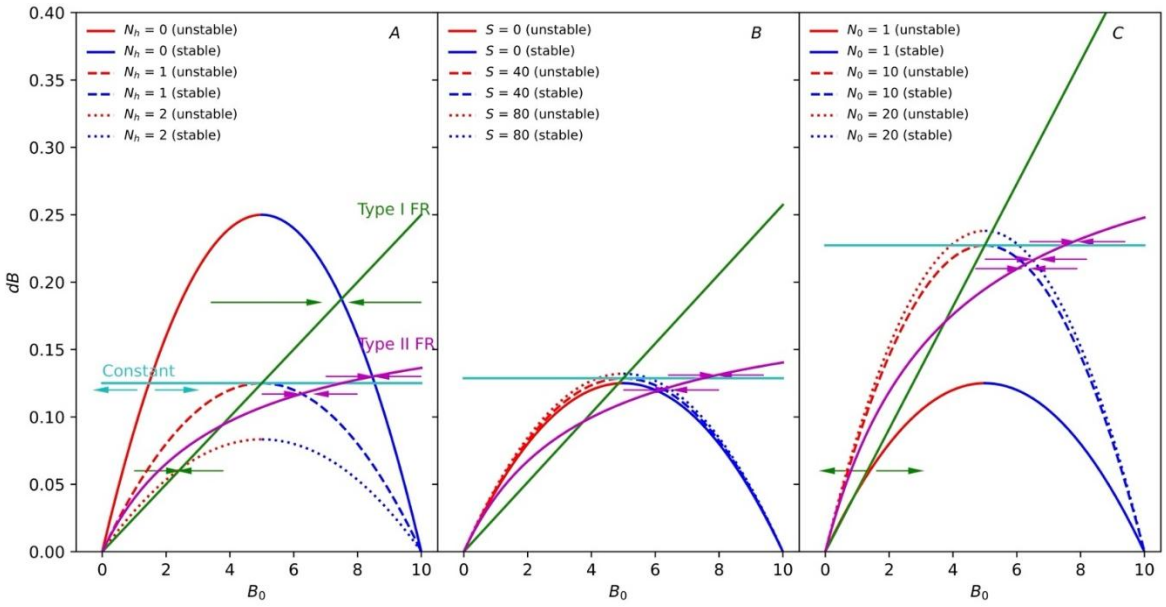

Figure 14. Derivative of B at different efficiencies in relation to N_h values (A), seeding rates (B), and initial conditions of N_0 (C). Red lines indicate unstable equilibria and blue lines stable equilibria. Black solid lines indicate constant extraction rates for $\mathrm{d}B = \mathrm{d}B_{\max}$ under the conditions of the coloured dashed lines, black dashed lines indicate proportional extraction (Holling's type-I functional response), and black dotted lines indicate Holling's type-II functional response extraction. The arrows show some equilibrium points, stable by convergent, and unstable by divergent arrows.

effect on the total biomass, and *iv)* biomass is removed by domestic herbivores, whose size is under the direct human control (i.e. based on a stocking rate decision). To achieve that goal, we split the population model into two different state variables: a) biomass (or raw abundance), which influences the growth rate of the population, and b) the number of individuals or vegetation cover, which influences the efficiency in consuming the resources of the environment.

As a result, the model simulates the populations along two independent variables: the number of individuals and total biomass. Biomass grows in a logistic way, being restricted by the carrying capacity of the system, whereas the number of individuals is limited by the average size. Hence, both variables are interconnected by a feedback loop, consisting of mutual restrictions. According to the model, the number of individuals is limited by biomass, so they can grow up to the limit where mortality and natality are balanced, and the net increase is zero. In turn, the number of individuals affects the efficiency at which the resources of the system are consumed by the population, limiting the growth rate of its biomass.

4.2. Human intervention

Human intervention has both a negative and a positive impact. On the one hand, negative intervention is represented as an indirect action, where the livestock removes biomass. That pattern attempts to simulate pastoral systems, where plant populations are measured in terms of biomass or vegetation cover, instead of the number of individuals (e.g., [39]–[42]). According to our approach, the number of individuals is associated positively with the surface covered [43]. This is a direct consequence of splitting the population size into two state variables, where one indicates the efficiency of consuming resources from the ecosystem. Populations of plant species covering a greater surface are capable of capturing resources more efficiently than a population concentrated more in a reduced space with the same total biomass [44].

On the other hand, a positive human intervention is represented by adding seeds or seedlings with zero or near-zero biomass, if compared to the carrying capacity. Adding seeds increases the spatial distribution and the number of individuals, thus increasing the efficiency in capturing the resources and, accordingly, the population size [45]. Given that the systems simulated are not subject to irrigation or fertilisation, no changes in carrying capacity are expected by human actions. Seeding of pastures is a frequent farming practice worldwide [46], which gained increased attention in the last decade in arid and semi-arid environments [46], [47]. Seeding replaces existing plants with more productive species [48] or increases the number of plants and their spatial coverage, such as in rangeland restoration programs [46]. Seedling planting also accelerates the recovery of rangeland populations, which is the rationale for its use in soil restoration initiatives [49], [50].

4.3. Global sensitivity and key parameters

The model shows robustness to initial conditions, consistently converging to a unique non-trivial equilibrium or extinction, without oscillatory or chaotic behaviours, even under nonlinear dynamics. This stability stems from the internal feedback loop between two distinct, yet interdependent, descriptors of the same population: biomass and number of individuals.

Among model parameters, the biomass equilibrium is most sensitive to the carrying capacity K_b, which governs the upper limit of biomass regardless of other influences. While other parameters modulate the rate or curvature of growth, K_b ultimately defines the system's long-term state.

In contrast, the equilibrium value of the number of individuals is most affected by the shape of the functional response curve, which defines how efficiently resources are captured per individual unit. This parameter influences both the slope and the curvature of the consumption function and therefore determines the speed and saturation level at which resource uptake approaches its maximum. As a consequence, it strongly affects the point where the consumption and recruitment curves intersect (see Figure 14), which is crucial for the establishment of a stable population size.

4.4. Model assumptions, limitations, and spatial scope

While the model captures key feedback in grazing systems with minimal complexity, it necessarily simplifies several ecological and management realities. Notably, all parameters (e.g., growth rates r_b, r_n, carrying capacity K_b) are held constant. In real systems, these parameters may vary due to climatic or anthropogenic drivers, such as rainfall, temperature, or land use change. Introducing temporal variability or stochasticity would increase realism, but at the cost of analytical tractability. Nevertheless, future studies could explore this through parametric sensitivity analyses or simulations under variable environments.

In its current form, the model also assumes that both extraction (grazing) and seeding occur continuously and deterministically. In practice, these are often seasonal or influenced by socio-economic constraints, introducing periodicity or stochastic forcing. Such extensions could be implemented via time-dependent functions $S(t)$ and $C(t)$, with system responses analysed through Fourier transforms or stochastic simulation methods.

The model remains spatially implicit. While spatial heterogeneity (e.g., fertility islands or patchy grazing) is an essential feature of many rangelands, its explicit representation requires detailed data, complex parameterisation, and computational cost. Moreover, the sessile nature of plants and their slow dispersal often make local feedback more relevant for seasonal or management timescales than large-scale spatial dynamics. Thus, the model is more prone to simplicity and generalisability than to spatial realism. Future work could hybridise this framework with spatially explicit models when spatial processes (e.g., water redistribution, erosion, or seed dispersal) dominate the system's behaviour.

The formulation of resource-use efficiency as a linear function of biomass-to-individual ratio $\left(\frac{B}{N} - Z_0\right)$ was chosen for mathematical simplicity. While nonlinear functions may better capture saturation, interference, or threshold effects, they also reduce the tractability and clarity of the results. Extensions with sigmoidal or hyperbolic efficiency functions could be tested numerically, notably in contexts where nonlinear effects are expected to be ecologically significant.

4.5. The dynamics of the model

Broadly, the dynamics of the system resemble the logistic models with extraction proposed by Schaeffer [34] and Noy-Meir [12], on which this model is based. Our contribution highlights that the number of individuals produces an effect on the short- and long-term dynamics as well. The stability of the system is close to the abovementioned logistic models with extraction, but with an additional parameter N_h. The initial conditions, in terms of $N_\mathrm{t} = 0$, and, in general, of the total population size, in terms of the number of individuals, affect the threshold or the unstable equilibrium point. The threshold separates the upper basin, in which the population stabilises at a finite positive value, and the other basin, in which the population converges to zero or becomes unsustainably low for the given extraction level.

4.6. Comparison with detailed biophysical approaches

This model can be considered an easier tool for simulating vegetation dynamics on extensive livestock production systems, being an alternative to complex biophysical models with several variables such as DSSAT [51] or DairyMod [52], to cite some examples. Besides their utility as managing tools or describing complex interactions between biophysical processes, complex models are often data-intensive and require the measurement of a large number of variables. Simpler models are more prone to generalise different types of systems or environments.

4.7. Methodological proposal for applicability on real data

Recently, new studies using field and remotely sensed data coupled with differential equation models have been supported by sophisticated estimation methods, such as Particle Filters or Sequential Montecarlo estimates, to describe the vegetation dynamics on rangelands [53]. These approaches, combined with this new model, can improve the results and allow a better understanding of vegetation dynamics in extensive livestock systems.

The number of individuals is a variable of difficult estimation from field surveys, but the use of new tools such as high-resolution images acquired by drones and coupled with computer vision allows measurements in larger areas [54]. As an alternative, vegetation cover is available in remotely sensed data [55], and it is a standard variable as well [41], [56]. While in some cases vegetation cover and biomass are considered interchangeable, they are conceptually different and the use of a different measure as a surrogate for biomass may generate misconceptions [57]. While these two variables are positively correlated, some differences might occur when the ecosystem is not in equilibrium [43]. In this case, even one variable might lag the other, depending on the intervention in the ecosystem, as shown in this study. Given that the main reason behind the separation of the number of individuals and biomass is to obtain a better measurement of the efficiency of the populations in reaching the resources, on a spatially spread population, without resorting to a spatially explicit model, for the purposes of this model, vegetation cover can be used to replace the number of individuals.

5. CONCLUSIONS

The model proposed in this study aims at simulating and studying the population dynamics of plants in extensive livestock systems, where population size is represented without increasing the overall complexity. By splitting the plant population size into biomass and number of individuals, we were able to add the effect of efficiency in consuming the resources in systems under continuous extraction without resorting to a spatially explicit model. This will allow further theoretical and field studies in which dynamical systems might be used to better understand measured population size data as a function of environmental variables.

Accordingly, we have provided a simplified yet effective framework for simulating plant population dynamics in extensive livestock systems. By separating biomass and the number of individuals, we capture the efficiency of resource use without resorting to spatially explicit models. This approach not only enhances our theoretical understanding of vegetation dynamics but also offers practical tools for rangeland management and restoration. Future research could explore the model's integration with remote sensing data and its application in diverse ecological and climatic contexts, further advancing sustainable rangeland management practices.

ACKNOWLEDGEMENTS

The authors are grateful to Dr Dardo R. López, for his input on these interesting ideas, for helping us to create the roots of this working group, and for introducing us to Noy-Meir's theory and modelling. O.A.B., M.H.E and D.V.P are funded by the Federal Council of Science and Technology, Argentina (COFECyT, Neuquén; CONVE-2019-12191100-APN-DDYGD-MECCYT). LR is funded by the European Commission under the Marie Sklodowska Curie Actions Postdoctoral Fellowship (MSCA-PF-2022) project '*PestFinder*' Grant no. 101102281.

AUTHORS' CONTRIBUTION

Conceptualisation: O.A.B., L.R., D.V.P., M.H.E.
Data curation: O.A.B.
Formal analysis: O.A.B., L.R.
Investigation: O.A.B., L.R.
Methodology: O.A.B., L.R.
Resources: O.A.B., L.R., D.V.P., M.H.E.
Software: O.A.B.
Writing – Original draft: O.A.B., L.R.
Writing – Editing and revision: O.A.B., L.R., D.V.P., M.H.E.

APPENDICES

Appendix A: Stability under constant extraction

We analyse the local stability of non-trivial equilibria in a coupled system describing total biomass $B(t)$ and the number of plant individuals $N(t)$, under constant extraction $C(t) = C > 0$. The governing equations are:

$$\begin{aligned} \frac{\mathrm{d}}{\mathrm{d}t} B(t) &= r_{\mathrm{b}} \frac{N(t)}{(N_{\mathrm{h}} + N(t))} B(t)\left(1 - \frac{B(t)}{K_{\mathrm{b}}}\right) - C \\ \frac{\mathrm{d}}{\mathrm{d}t} N(t) &= r_{\mathrm{n}} \left(\frac{B(t)}{N(t)} - Z_0\right) N(t) + S\,. \end{aligned} \tag{A1}$$

We look for non-trivial equilibria (B^*, N^*) satisfying

$$0 = r_{\mathrm{b}} \frac{N^*}{N_{\mathrm{h}} + N^*} B^* \left(1 - \frac{B}{K_{\mathrm{b}}}\right) - C \tag{A2}$$

$$0 = r_{\mathrm{n}} \left(\frac{B^*}{N^*} - Z_0\right) N^* + S\,. \tag{A3}$$

The Jacobian (B^*, N^*) is:

$$J(B^*, N^*) = \begin{pmatrix} \dfrac{\partial f_{\mathrm{B}}}{\partial B} & \dfrac{\partial f_{\mathrm{B}}}{\partial N} \\ \dfrac{\partial f_{\mathrm{N}}}{\partial B} & \dfrac{\partial f_{\mathrm{N}}}{\partial N} \end{pmatrix}, \tag{A4}$$

with

$$\frac{\partial f_{\mathrm{B}}}{\partial B} = r_{\mathrm{b}} \left(\frac{N^*}{N_{\mathrm{h}} + N^*}\right)\left(1 - \frac{2\,B^*}{K_{\mathrm{b}}}\right) \tag{A5}$$

$$\frac{\partial f_{\mathrm{B}}}{\partial N} = r_{\mathrm{b}} B^* \left(1 - \frac{B^*}{K_{\mathrm{b}}}\right)\left(\frac{N_{\mathrm{h}}}{(N_{\mathrm{h}} + N^*)^2}\right) \tag{A6}$$

$$\frac{\partial f_{\mathrm{N}}}{\partial B} = r_{\mathrm{n}} \tag{A7}$$

$$\frac{\partial f_{\mathrm{N}}}{\partial N} = -r_{\mathrm{n}}\left(Z_0 - \frac{B^*}{N^*}\right). \tag{A8}$$

Stability requires:

$$tr(J) = J_{11} + J_{22} < 0$$

$$\det(J) = J_{11}J_{22} - J_{12}J_{21} > 0\,.$$

Appendix B: Stability under type-II functional response extraction

Let us consider the extraction described by a type-II functional response:

$$C(B) = \frac{a\,B}{h + B}, \tag{A9}$$

with $a > 0$ the maximum extraction rate and $h > 0$ the half-saturation constant. The governing equations are:

$$\begin{aligned}\frac{\mathrm{d}}{\mathrm{d}t}B(t) &= r_{\mathrm{b}}\frac{N(t)}{\left(N_{\mathrm{h}} + N(t)\right)}B(t)\left(1 - \frac{B(t)}{K_{\mathrm{b}}}\right) \\ &\quad - \frac{a\,B}{h + B} \\ \frac{\mathrm{d}}{\mathrm{d}t}N(t) &= r_{\mathrm{n}}\left(\frac{B(t)}{N(t)} - Z_0\right)N(t) + S\,.\end{aligned} \tag{A10}$$

The equilibrium conditions are

$$0 = r_{\mathrm{b}}\frac{N^*}{N_{\mathrm{h}} + N^*}B^*\left(1 - \frac{B}{K_{\mathrm{b}}}\right) - \frac{a\,B^*}{h + B^*} \tag{A11}$$

$$0 = r_{\mathrm{n}}\left(\frac{B^*}{N^*} - Z_0\right)N^* + S \tag{A12}$$

and the Jacobian

$$\frac{\partial f_B}{\partial B} = r_{\mathrm{b}}\left(\frac{N^*}{N_{\mathrm{h}} + N^*}\right)\left(1 - \frac{2\,B^*}{K_{\mathrm{b}}}\right) - \frac{a\,h}{(h + B^*)^2} \tag{A13}$$

$$\frac{\partial f_B}{\partial N} = r_{\mathrm{b}}\,B^*\left(1 - \frac{B^*}{K_{\mathrm{b}}}\right)\left(\frac{N_{\mathrm{h}}}{(N_{\mathrm{h}} + N^*)^2}\right) \tag{A14}$$

$$\frac{\partial f_N}{\partial B} = r_{\mathrm{n}} \tag{A15}$$

$$\frac{\partial f_N}{\partial N} = -r_{\mathrm{n}}\left(Z_0 - \frac{B^*}{N^*}\right). \tag{A16}$$

Reduced biomass dynamics

Simplified model:

$$\frac{\mathrm{d}}{\mathrm{d}t}B(t) = r_{\mathrm{b}}\,B(t)\left(1 - \frac{B(t)}{K_{\mathrm{b}}}\right) - \frac{a\,B}{h + B}, \tag{A17}$$

with equilibrium conditions given by

$$\left[r_{\mathrm{b}}\left(1 - \frac{B}{K_{\mathrm{b}}}\right)(h + b) - a\right] = 0\,. \tag{A18}$$

Let us define

$$f(B) = r_{\mathrm{b}}\left(1 - \frac{B}{K_{\mathrm{b}}}\right)(h + b) - a\,. \tag{A19}$$

If $a > f(B)$, biomass collapses. Otherwise, one or two positive equilibria exist. The Jacobian in this case is:

$$J(B^*) = r\left(1 - \frac{2\,B^*}{K}\right) - \frac{a\,h}{(h + B)^2}. \tag{A20}$$

Appendix C: Conceptual conclusions

- Both constant and type-II extraction reduce equilibrium biomass. Collapse occurs if extraction exceeds regenerative capacity.
- External input $S > 0$ helps to sustain N^*, buffering collapse risk.
- Type-II extraction introduces non-linearities; critical extraction rate depends on a and h.
- Local stability follows from the Jacobian trace and determinant. Collapse can be anticipated by evaluating these conditions.

REFERENCES

[1] I. Hanski, Single-species metapopulation dynamics: concepts, models and observations, Biological Journal of the Linnean Society, vol. 42, issue 1–2, 1991, pp. 17–38. DOI: 10.1111/j.1095-8312.1991.tb00549.x

[2] B. Oborny, Géza Meszéna, György Szabó, Dynamics of populations on the verge of extinction, Oikos, vol. 109, issue 2, 2005, pp. 291–296. DOI: 10.1111/j.0030-1299.2005.13783.x

[3] M. Petit, Success in agricultural transformation: What it means and what makes it happen, European Review of Agricultural Economics, vol. 39, issue 5, 2012, pp. 882–884. DOI: 10.1093/erae/jbs035

[4] J. Zhang, M. D. Smith, Estimation of a generalized fishery model: A two-stage approach, Review of Economics and Statistics, vol. 93, issue 2, 2011, pp. 690–699. DOI: 10.1162/REST_a_00075

[5] J. P. Ritten, C. T. Bastian, W. M. Frasier, Economically optimal stocking rates: A bioeconomic grazing model, Rangeland Ecology & Management, vol. 63, issue 4, 2010, pp. 407–414. DOI: 10.2111/08-253.1

[6] F. B. Hanson, D. Ryan, Optimal harvesting with both population and price dynamics, Mathematical Biosciences, vol. 148, issue 2, 1998, pp. 129–146. DOI: 10.1016/S0025-5564(97)10011-6

[7] T. Kristensen, K. Søegaard, I. S. Kristensen, Management of grasslands in intensive dairy livestock farming, Livestock Production Science, vol. 96, 2005, pp. 61–73.

[8] J. F. Reynolds, D. M. Stafford Smith, E. F. Lambinet, (+ another 14 authors) Global desertification: building a science for dryland development, Science, vol. 316, issue 5826, 2007, pp. 847–851. DOI: 10.1126/science.1131634

[9] J. M. Paruelo, H. E. Epstein, W. K. Laurenroth, I. Burke, ANPP estimates from NDVI for the central grassland region of the United States, Ecology, vol. 78, issue 3, 1997, pp. 953–958.

[10] H. Ren, G. Zhou, Estimating green biomass ratio with remote sensing in arid grasslands, Ecological Indicators, vol. 98, 2019, pp. 568–574. DOI: 10.1016/j.ecolind.2018.11.043

[11] P. Chesson, Predator-prey theory and variability, Annu. Rev. Ecol. Syst., vol. 9, issue 1, 1978, pp. 323–347. DOI: 10.1146/annurev.es.09.110178.001543

[12] I. Noy-Meir, Stability of grazing systems: An application of predator-prey graphs, The Journal of Ecology, vol. 63, issue 2, 1975, p. 459.
DOI: 10.2307/2258730
[13] I. Noy-Meir, Rotational grazing in a continuously growing pasture: A simple model, Agricultural Systems, vol. 1, issue 2, 1976, pp. 87–112.
DOI: 10.1016/0308-521X(76)90009-3
[14] I. Noy-Meir, Grazing and production in seasonal pastures: analysis of a simple model, The Journal of Applied Ecology, vol. 15, issue 3, 1978, p. 809.
DOI: 10.2307/2402778
[15] H. Fort, F. Dieguez, V. Halty, J. M. S0ares de Lima, Two examples of application of ecological modeling to agricultural production: Extensive livestock farming and overyielding in grassland mixtures, Ecological Modelling, vol. 357, 2017, pp. 23–34.
DOI: 10.1016/j.ecolmodel.2017.03.023
[16] F. Dieguez Cameroni, H. Fort, Towards scientifically based management of extensive livestock farming in terms of ecological predator-prey modeling, Agricultural Systems, vol. 153, 2017, pp. 127–137.
DOI: 10.1016/j.agsy.2017.01.021
[17] M. Segoli, E. D. Ungar, M. Shachak, Fine-scale spatial heterogeneity of resource modulation in semi-arid "Islands of Fertility", Arid Land Research and Management, vol. 26, issue 4, 2012, pp. 344–354.
DOI: 10.1080/15324982.2012.694397
[18] D. J. Tongway, J. A. Ludwig, Heterogeneity in arid and semiarid lands, in Ecosystem Function in Heterogeneous Landscapes, G. M. Lovett, M. G. Turner, C. G. Jones, K. C. Weathers, A c. di, New York, NY: Springer New York, 2005, pp. 189–205.
DOI: 10.1007/0-387-24091-8_10
[19] R. Bastiaansen, O. Jaïbi, V. Deblauwe, (+ another 7 authors), Multistability of model and real dryland ecosystems through spatial self-organization, Proc. Natl. Acad. Sci. U.S.A., vol. 115, issue 44, 2018, pp. 11256–11261.
DOI: 10.1073/pnas.1804771115
[20] S. Schwinning, A. J. Parsons, A spatially explicit population model of stoloniferous N-fixing legumes in mixed pasture with grass, The Journal of Ecology, vol. 84, issue 6, 1996, p. 815.
DOI: 10.2307/2960554
[21] M. A. Altieri, Agroecology, small farms, and food sovereignty, Mon. Rev., vol. 61, issue 3, 2009, p. 102.
DOI: 10.14452/MR-061-03-2009-07_8
[22] A. E. De Villalobos, D. V. Peláez, O. R. Elia, Factors related to establishment of *Prosopis caldenia* Burk. seedlings in central rangelands of Argentina, Acta Oecologica, vol. 27, issue 2, 2005, pp. 99–106.
DOI: 10.1016/j.actao.2004.10.001
[23] S. P. Hardegree, J. T. Abatzoglou, M. W. Brunson, (+ another 7 authors), Weather-centric rangeland revegetation planning, Rangeland Ecology & Management, vol. 71, issue 1, 2018, pp. 1–11.
DOI: 10.1016/j.rama.2017.07.003
[24] M. M. W. Abu-Zanat, A. K. Al-Ghaithi, M. W. Akash, Effect of Planting Atriplex seedlings in micro-catchments on attributes of natural vegetation in arid rangelands, Journal of Arid Environments, vol. 180, 2020, p. 104199.
DOI: 10.1016/j.jaridenv.2020.104199
[25] L. Gallego, R. A. Distel, R. Camina, R. M. Rodríguez Iglesias, Soil phytoliths as evidence for species replacement in grazed rangelands of central Argentina, Ecography, vol. 27, issue 6, 2004, pp. 725–732.
DOI: 10.1111/j.0906-7590.2005.03964.x
[26] S. Ul-Allah, A. A. Khan, T. Fricke, A. Buerkert, M. Wachendorf, Effect of fertiliser and irrigation on forage yield and irrigation water use efficiency in semi-arid regions of Pakistan, Ex. Agric., vol. 51, issue 4, 2015, pp. 485–500.
DOI: 10.1017/S001447971400043X
[27] M. Sketch, A. A. Dayer, A. L. Metcalf, Western ranchers' perspectives on enablers and constraints to flood irrigation, Rangeland Ecology & Management, vol. 73, issue 2, 2020, pp. 285–296.
DOI: 10.1016/j.rama.2019.12.003
[28] O. Bruzzone, D. A. Castillo, E. S. Villagra, Growth curve of early-weaned Hereford calves in a semidesert temperate zone (Patagonia, Argentina), Livestock Science, vol. 259, 2022, p. 104908.
DOI: 10.1016/j.livsci.2022.104908
[29] E. D. Ungar, Perspectives on the concept of rangeland carrying capacity, and their exploration by means of Noy-Meir's two-function model, Agricultural Systems, vol. 173, 2019, pp. 403–413.
DOI: 10.1016/j.agsy.2019.03.023
[30] C. Donald, Competition among pasture plants. II. The influence of density on flowering and seed production in annual pasture plants., Aust. J. Agric. Res., vol. 5, issue 4, 1954, p. 585.
DOI: 10.1071/AR9540585
[31] N. Stollenwerk, M. Aguiar, B. W. Kooi, Modelling Holling type II functional response in deterministic and stochastic food chain models with mass conservation, Ecological Complexity, vol. 49, 2022, p. 100982.
DOI: 10.1016/j.ecocom.2022.100982
[32] L. Michaelis, M. M. L. Menten, Die Kinetik der Invertinwirkung, Biochemistry, vol. 49, 1913, pp. 333–369.
[33] A. Oaten, W. W. Murdoch, Functional response and stability in predator-prey systems, The American Naturalist, vol. 109, issue 967, 1975, pp. 289–298.
DOI: 10.1086/282998
[34] M. B. Schaefer, Some aspects of the dynamics of populations important to the management of the commercial marine fisheries, vol. 53, 1991, pp. 253–279.
[35] L. A. Real, The kinetics of functional response, The American Naturalist, vol. 111, issue 978, 1977, pp. 289–300.
DOI: 10.1086/283161
[36] J. Barcroft, A. V. Hill, The nature of oxyhaemoglobin, with a note on its molecular weight. The Journal of Physiology, 39, pp. 411–428.
DOI: 10.1113/jphysiol.1910.sp001350
[37] E. van Leeuwen, Å. Brännström, V. A. Jansen, U. Dieckmann, A. G. Rossberg, A generalized functional response for predators that switch between multiple prey species, Journal of theoretical biology, 328, pp. 89–98.
DOI: 10.1016/j.jtbi.2013.02.003
[38] C. R. Harris. K. J. Millmann, S J. van der Walt, (+ another 23 authors), Array programming with NumPy, Nature, vol. 585, issue 7825, 2020, pp. 357–362.
DOI: 10.1038/s41586-020-2649-2
[39] O. Bruzzone, Vegetation Dynamics Paper on GitHub. Online [Accessed 3 September 2025]
https://github.com/okktawio/Vegetation_Dynamics_Paper
[40] P. Flombaum, O. E. Sala, A non-destructive and rapid method to estimate biomass and aboveground net primary production in arid environments, Journal of Arid Environments, vol. 69, issue 2, 2007, pp. 352–358.
DOI: 10.1016/j.jaridenv.2006.09.008
[41] C. Redjadj, A. Duparc, S. Lavorel, (+ another 5 authors), Estimating herbaceous plant biomass in mountain grasslands: a comparative study using three different methods, Alp Botany, vol. 122, issue 1, 2012, pp. 57–63.
DOI: 10.1007/s00035-012-0100-5
[42] D. R. López, M. A. Brizuela, P. Willems, M. R. Aguiar, G. Siffredi, D. Bran, Linking ecosystem resistance, resilience, and stability in steppes of North Patagonia, Ecological Indicators, vol. 24, 2013, pp. 1–11.
DOI: 10.1016/j.ecolind.2012.05.014
[43] F. A. Funk, G. Peter, C. V. Leder, A. Loydi, A. Kröpfl, R. A. Distel, The impact of livestock grazing on the spatial pattern of vegetation in north-eastern Patagonia, Argentina, Plant Ecology &

Diversity, vol. 11, issue 2, 2018, pp. 219–227.
DOI: 10.1080/17550874.2018.1473519
[44] T. Han, H. Lu, Y. Lü, B. Fu, Assessing the effects of vegetation cover changes on resource utilization and conservation from a systematic analysis aspect, Journal of Cleaner Production, vol. 293, 2021, p. 126102.
DOI: 10.1016/j.jclepro.2021.126102
[45] D. R. López, L. Cavallero, P. Willems, B. T. Bestelmeyer, M. A. Brizuela, Degradation influences equilibrium and non-equilibrium dynamics in rangelands: implications in resilience and stability, Applied Vegetation Science, vol. 25, issue 3, 2022, p. e12670.
DOI: 10.1111/avsc.12670
[46] C. C. Small, D. Degenhardt, Plant growth regulators for enhancing revegetation success in reclamation: A review, Ecological Engineering, vol. 118, 2018, pp. 43–51.
DOI: 10.1016/j.ecoleng.2018.04.010
[47] M. Louhaichi, S. Hassan, A. M. Missaoui, (+ another 5 authors), Impacts of bracteole removal and seeding rate on seedling emergence of halophyte shrubs: implications for rangeland rehabilitation in arid environments, Rangel. J., vol. 41, issue 1, 2019, p. 33.
DOI: 10.1071/RJ18064
[48] D. Rodrigues, L. P. Barra, M. Lobosco, F. Bastos, Analysis of Turing Instability for Biological Models, in Lecture Notes in Computer Science (including subseries Lecture Notes in Artificial Intelligence and Lecture Notes in Bioinformatics), vol. 8584 LNCS, issue PART 6, 2014, pp. 576–591.
DOI: 10.1007/978-3-319-09153-2_43
[49] J. M. Peralta, M. Dietrich, R. C. Gil, A. Sarmiento, G. Becker, Red de ensayos territoriales para la provincia de Neuquen: "Agricultura para la ganadería", Documento de Trabajo N° 11. Actividad Pecuaria en la Provincia del Neuquén, 2013. [In Spanish]
[50] C. A. Busso, D. R. Pérez, Opportunities, limitations and gaps in the ecological restoration of drylands in Argentina, Annals of Arid Zone, vol. 57, issue 3, 2018, pp. 191–200.
[51] D. A. Pyke, T. A. Wirth, J. L. Beyers, Does seeding after wildfires in rangelands reduce erosion or invasive species?, Restoration Ecology, vol. 21, issue 4, 2013, pp. 415–421.
DOI: 10.1111/rec.12021
[52] J. W. Jones, G. Hoogenboom, C. H. Porter, (+ another 7 authors), The DSSAT cropping system model, European Journal of Agronomy, vol. 18, 2003, pp. 235–265.
DOI: 10.1016/S1161-0301(02)00107-7
[53] I. R. Johnson, D. F. Chapman, V. O. Snow, (+ another 4 authors), DairyMod and EcoMod: biophysical pasture-simulation models for Australia and New Zealand, Aust. J. Exp. Agric., vol. 48, issue 5, 2008, p. 621.
DOI: 10.1071/EA07133
[54] O. A. Bruzzone, D. V. Perri, M. H. Easdale, Vegetation responses to variations in climate: A combined ordinary differential equation and sequential Monte Carlo estimation approach, Ecological Informatics, vol. 73, 2023, p. 101913.
DOI: 10.1016/j.ecoinf.2022.101913
[55] B. Hosseiny, H. Rastiveis, S. Homayouni, An automated framework for plant detection based on deep simulated learning from drone imagery, Remote Sensing, vol. 12, issue 21, 2020, p. 3521.
DOI: 10.3390/rs12213521
[56] L. Gao, X. Wang, B. A. Joonson, (+ another 5 authors), Remote sensing algorithms for estimation of fractional vegetation cover using pure vegetation index values: A review, ISPRS Journal of Photogrammetry and Remote Sensing, vol. 159, 2020, pp. 364–377.
DOI: 10.1016/j.isprsjprs.2019.11.018
[57] D. J. Tongway, J. A. Ludwig, Vegetation and soil patterning in semi-arid mulga lands of Eastern Australia, Australian Journal of Ecology, vol. 15, issue 1, 1990, pp. 23–34.
DOI: 10.1111/j.1442-9993.1990.tb01017.x
[58] A. Chiarucci, J. B. Wilson, B. J. Anderson, V. De Dominicis, Cover versus biomass as an estimate of species abundance: does it make a difference to the conclusions?, J Vegetation Science, vol. 10, issue 1, 1999, pp. 35–42.
DOI: 10.2307/3237158